A Genome-wide CRISPR screen unveils the endosomal maturation protein WDR91 as a promoter of productive ASO activity in melanoma

Grégory Menchon[1], Aris Gaci[2], Antti Matvere[1], Marc Aubry[1], Aurélien Bore[3], David Gilot[1,4], Aurélie Goyenvalle[2] and Rémy Pedeux[1*]

[1] INSERM, OSS, UMR_S 1242, Univ. Rennes, 35000, Rennes, France

[2] Université Paris-Saclay, UVSQ, Inserm, END-ICAP, 78000 Versailles, France

[3] CRISPR'iT Genetic Platform Screening, Institut Curie, INSERM U934, CNRS UMR3215, 75005, Paris, France

[4] Mechanistic & Structural Biology, Discovery Sciences, R&D, AstraZeneca, SE-48183, Mölndal, Sweden

*Correspondence should be addressed to R.P. (remy.pedeux@univ-rennes.fr)

INSERM, OSS, UMR_S 1242, Univ. Rennes, 35000, Rennes, France

Tel : +33(0)223234702

SHORT TITLE

A CRISPR screen unveils ASO activity modulators

ABSTRACT

Antisense oligonucleotides (ASOs) belong to promising therapeutics for the treatment of neurologic, muscular and metabolic disorders. Several ASOs have been approved so far and more than a hundred clinical trials are currently underway covering a dozen therapeutic areas. Yet, the mechanisms of internalization and cell trafficking of these molecules remain poorly understood. Moreover, with only a small fraction of ASOs reaching the correct cellular compartment following systemic delivery, the majority of targeted diseases requires recurrent injections of ASOs. A deeper understanding of these mechanisms would guide the improvement of their potency and thus, reduce the amount of delivered ASOs and their potential side-effects. Here, using a CRISPR screen, we investigated intracellular proteins involved in ASOs efficiency using a whole genome approach and identified several potential regulators which could significantly impact ASOs potency in melanoma cells. We validated WD Repeat Domain 91 (WDR91), a regulator of endosomal maturation, as a modulator whose depletion significantly inhibits ASO productive activity. This study provides the first list of ASO modulators using a biologically relevant assay to estimate the role of these proteins. In conclusion, these data could lead to a better understanding of the mechanisms favoring productive uptake or improved endosomal escape of ASOs.

44 **INTRODUCTION**

45 Antisense Synthetic Oligonucleotides (ASOs) belong to a class of attractive therapeutic
46 compounds for numerous diseases. ASOs modulate cellular target gene expression through
47 Watson-Crick binding to complementary RNA molecules and, according to their type, act by
48 either promoting a RNAse-H1 mediated RNA degradation (Gapmers - GMs) or through a steric
49 blocking mechanism (mixmers and target site blockers – TSBs) leading to three major modes
50 of action: inhibition or activation of gene-expression and splicing modulation.[1] ASOs have been
51 developed for the treatment of different genetic disorders and they can be translated to
52 personalized therapies.[2] ASOs are specially taken up by fast growing cells[3] and, among
53 numerous advantages, bypass the current bottleneck regarding the targets that are considered
54 undruggable with traditional small molecule inhibitors.[4] Several ASOs are currently approved
55 by the Food and Drug Administration (FDA) for genetic and rare diseases[5,6] and several phase
56 II and III studies are ongoing in the oncology therapeutic area.[7]

57 Although ASOs promise a great leap forward in future cancer treatments, their utilization
58 suffers from major hurdles. Among them, a lack of tissue specific targeting,[8,9] poor cellular
59 uptake[10] and the need to escape from the endo-lysosomal pathway to exert their role in either
60 the cytoplasm or nucleus of the cells.[11,12] Moreover, the mechanisms of internalization, cell
61 trafficking and action of these molecules remain poorly understood. A small fraction of ASO
62 reaching the right cellular compartment and target following systemic delivery[13,14] leads to
63 treatments consisting of high doses, recurrent injections and thus, significant accumulation in
64 other non-targeted cells and organs with consecutive toxicities.[15] It is therefore essential to
65 better understand the fate of internalized ASOs and their intracellular route and mode of action.
66 Such deeper characterization in different cell lines and with different ASO types and
67 chemistries would help in the rational design and improvement of therapeutic ASO strategies
68 in future clinical applications. Several studies have demonstrated that the fate of internalized

69 phosphorothioate (PS)-containing ASOs was determined by intracellular interacting
70 proteins.[16,17,18] Even if a clear mechanism is still to be fully understood, around 80 intracellular
71 proteins have been identified and this protein interactome appears to influence the
72 pharmacological activities and potential toxicities of PS-ASOs by acting on their uptake and
73 distribution. It is also worth noting that many other proteins that bind to ASOs have no effect
74 on their activity. PS-ASOs are internalized and processed through the endocytic pathway,[3,19]
75 but proteins can modulate endosome traffic and maturation without interacting directly with
76 oligonucleotides. Previous studies have investigated the modulation of intracellular pathways
77 to increase the productive delivery and activity of oligonucleotides and to further unveil the
78 critical molecular factors that contribute to nucleic acids pharmacological effects.[20] Among
79 these, modulation of endocytic recycling,[21,22] multivesicular bodies' (MVBs) fusion with
80 lysosomes,[23] endosomal escape[24] and nuclear shuttling[25,26] were explored. All these strategies
81 involve the use of either genetic or non-genetic perturbations and have proven to be successful
82 in many *in vitro* and *in vivo* studies. ASO-interacting proteins have been mostly characterized
83 by *in vitro* studies using pull-down experiments on cell lysates[27,28] but such method lacks
84 physiological relevance as the intracellular membrane's integrity is not preserved and could
85 lead to many binding artefacts. Furthermore, pull-down studies may highlight some important
86 ASOs protein modulators but only allow the identification of direct interactants. To circumvent
87 these issues other authors recently used proximity biotinylation assay to highlight
88 oligonucleotides interactome in living cells and in pharmacologically relevant conditions.[29]

89 Clustered Regularly Interspaced Short Palindromic Repeats (CRISPR) screen is a powerful
90 genetic perturbation method that can be used for functional genomic studies, by activating or
91 silencing genes.[30] Then, it can be implemented to identify ASOs direct and indirect modulators
92 in a more physiological state and preserving the cell membrane's integrity. This technique was
93 implemented in different studies to investigate modulators of dsRNAs,[31] Antibody-Drug

Conjugates (ADCs)[32] or encapsulated mRNAs,[33] but to our knowledge, only one study describes such a functional genomic screen (CRISPR gene activation) to uncover factors enhancing ASOs activity.[34]

In the present work, we used a genome-wide CRISPR screen strategy (CRISPR knockout), to uncover proteins that modulate the potency of an anti-proliferative tricyclo-DNA (tcDNA) based-ASO in a melanoma cell line (501Mel). The generation of the parental knockout cell library was performed such as every single cell had a unique depleted coding gene. The library was then treated with ASO, and sequencing was performed on the surviving (enriched or depleted) cells. This analysis highlighted several candidates of interest (95 activators and 55 inhibitors). From the top candidates, the robustness of our assay also allowed to highlight the proteins Ras-related protein Rab5C (Rab5C) and Component of Oligomeric Golgi Complex 8 (COG8) which are known positive regulators of ASOs productive trafficking and activity.[35,36] We unveiled the endosomal maturation protein WDR91 as a strong positive regulator of the tcDNA based-ASO activity in this cell line. Activity modulation by WDR91 was validated together with Annexin A2 (ANXA2), a well characterized endosomal protein which promotes ASOs trafficking and productive activity in different cell lines.[37] The impact of WDR91 was validated using two different ASO chemistries but was not validated on a splice switching ASO in a muscle cell line, highlighting a cell type-dependent effect. Finally, this work provides a detailed source of potential positive and negative regulators of ASO activity, coming from an unbiased screen and with a strong physiological relevance.

118 **RESULTS**

119 **Development and *in vitro* validation of a tcDNA-ASO to inhibit 501Mel cells proliferation**
120 **with a target-site blocking mechanism**

121 Previous work aiming at masking a microRNA (miRNA) target site on a microRNA sponge
122 (*TYRP1* mRNA) led to the test and validation of a commercially-designed Locked Nucleic Acid
123 (LNA) TSB (named TSB-T3 for Target-Site Blocking – T3). In this study, TSB-T3 significantly
124 induced the reduction of melanoma tumor growth *in vitro* and in 501Mel xenografts.[38] This
125 ASO was validated in five different cell lines and had a dose-response anti-proliferative
126 activity. TSB-T3 exerts its ASO masking activity by preventing the sequestration of the miR-
127 16 tumor suppressor by *TYRP1* mRNA and redirecting it towards its target-RNAs, to induce
128 their decay and subsequently reduce tumor proliferation (**Figure 1A**).[39] This miRNA
129 displacement mediated by a Target Site Blocker ASO represents a relevant assay to investigate
130 the proteins involved in ASOs efficiency. The ASO blocking activity is directly monitored
131 through an anti-proliferative effect, which has been validated *in vivo*.

132 In the present study, we decided to look for protein modulators of an ASO with a clinically
133 relevant chemistry. We thus designed and evaluated a new TSB-T3 with the same sequence but
134 with a full tcDNA chemistry and phosphorothioate (PS) backbone (tcT3). This class of
135 conformationally constrained ASO displays enhanced binding properties to DNA and RNA as
136 well as unique pharmacological properties and unprecedented uptake by many tissues after
137 systemic administration.[40,41]

138 To compare both chemistries, 501Mel cells were reverse-transfected in 96-well plates with
139 either the LNA- or the tcDNA-ASO (named respectively T3 and tcT3). We deliberately used
140 high doses of ASOs (up to 70nM) as their blocking activity is based on the displacement of a
141 sequestered miR-16 by *TYRP1* mRNA which is, besides, highly expressed in melanoma cells

142 (with around 3200 copies per cell).[38] After 72h, the cell density was measured by colorimetric
143 assay and normalized to a control ASO treatment (C1 or tcC1). As expected, we confirmed
144 previous results with the commercial reagent. Both T3 and tcT3 ASOs showed a dose-response
145 anti-proliferative activity and, interestingly, the tcDNA chemistry improved the ASO potency
146 at low doses (**Figure 1B**). This tcDNA-ASO was selected for the subsequent screening
147 experiment.

148

149 **Genome-wide pooled sgRNA library generation, knockout library treatment with tcDNA-**
150 **ASOs and NGS sequencing**

151 The CRISPR-knockout cell library was generated by transducing 501Mel cells with a pooled
152 lentiviral library which contains the Cas9 and sgRNAs targeting 19.114 human coding genes.
153 This lentivirus library contains 4 different guides per coding gene (total of 76.441 sgRNAs) and
154 1000 non-targeting control sgRNAs. A multiplicity of infection (MOI) of 0.4 was selected to
155 ensure that only few cells are transduced with more than one sgRNA and avoid unspecific
156 screening results.[42] With 76.441 sgRNAs and a desired coverage of at least 400 cells per guide,
157 a total of 32 million cells have been transduced and maintained during the screen.

158 After transduction, the cells were positively selected with antibiotic, expanded and
159 subsequently transfected with either the tcT3 or -C1 ASOs. A final ASO concentration of 50nM
160 was selected based on the former dose-response experiment which showed that the anti-
161 proliferative effect reached a plateau at this dose (**Figure 1B**). The treatment was performed
162 for three days. After this period, the difference in cell density between the treated and control
163 conditions was greater than 50%.

164 At the end of treatment, the cells were expanded, pooled and a pellet of 100 million cells per
165 condition was used for genomic DNA (gDNA) extraction and PCR amplification of the

166 integrated sgRNAs in the 3 conditions (non-treated parental cell bank, tcT3 treated and tcC1
167 treated). The global workflow is depicted in **Figure 2A**.

168 After amplicons sequencing by NGS, a quality check was performed and only 115 sgRNAs
169 were not detected over 76.441 in our cell library (0.15%), which validated proper conditions
170 before ASOs treatment. The normalized reads count in each control and therapeutic ASO
171 condition were plotted and provided a mean of 400-500 reads per guide as expected (**Figure**
172 **2B**).

173 The sequenced sgRNAs coming from the pool of surviving cells after ASO treatment provided
174 information regarding the enriched or depleted ones. Thus, by comparing the sgRNAs
175 enrichment or depletion in treated *versus* control condition and for each gene, we sought to
176 identify proteins potentially involved in the regulation of ASO uptake, trafficking, release and
177 guidance to their RNA-target in this melanoma cell line (**Figure 2C**).

178

179 **Identification of tcT3 ASO activity regulators in 501Mel cells**

180 To identify proteins that could impact the tcT3 activity in 501Mel cell line, the NGS sequencing
181 raw data accounting for the total number of sgRNA reads per gene and per sample were
182 analyzed as follows. First, we used MAGeCK count to collect sgRNA read count information
183 from the tcC1- and tcT3-treated cells sequencing files. Then, we used MA Plots to score and
184 identify candidates based on the sgRNA read abundance (A value) and the read counts ratio
185 between the treated and the control condition (M value: fold change - FC). M and A values
186 were computed for each of the 4 sgRNAs targeting each individual gene (**Figure 3A**). From the
187 MA plots, top activator and inhibitor candidates were extracted after using a defined M cutoff
188 for each sgRNA per gene. The **figure 3B** represents MA plot examples from selected activator
189 and inhibitor candidates with applied M cutoff and with 4 (GGTLC2) or 2 relevant sgRNAs

190 (WDR91). Because of a short time of treatment (72h), a minimum FC of 1.5 was fixed between
191 the tcT3 and tcC1 read counts to highlight the best hits (activator candidates: fold change tcT3
192 read counts *vs* tcC1 read counts ≥ 1.5; inhibitor candidates: fold change tcC1 read counts *vs*
193 tcT3 read counts ≥ 1.5) (Candidates examples in **Figure 3C**). We opted for a short time of
194 treatment to avoid guide selection bias.

195 Several sgRNAs targeting the same gene might not have a consistent behavior. However, the
196 Brunello library has been designed with optimized sgRNAs and is known to outperform other
197 knockout libraries.[43] Indeed, the robustness of this library has already been demonstrated with
198 the ability to identify reliable candidates with only 2 effective sgRNAs per gene.[43] We thus
199 extracted activator and inhibitor candidates considering two, three or four out of four guides
200 meeting the defined M (FC) and A selection criteria.

201 As shown in **Figure 4A and B** (and in **Table 1**), this cutoff allowed to highlight a set of 95
202 activator candidates and 55 inhibitors. Regarding the activators, 5 genes had their 4 respective
203 sgRNAs fulfilling the corresponding criteria; 28 genes had 3 effective sgRNAs and 62 genes
204 had 2 effective sgRNAs over 4. From the inhibitors, 3, 7 and 45 genes had 4, 3 and 2 effective
205 sgRNAs, respectively. Each of the candidates have been represented by an average FC value
206 but a detailed table of each sgRNA and their respective M, A and FC values is available in
207 **Table 1**.

208 Gene set enrichment analysis using PANGEA (Pathway, Network and Gene-set Enrichment
209 Analysis) allowed to classify the activator and inhibitor candidates based on the cellular
210 component gene ontology (**Supplemental Figures S1 and S2**).[44] Interestingly, the activator
211 candidates with the highest fold enrichment are mainly clustered within proteins belonging to
212 the peroxisome and mitochondria compartments. Inhibitor candidates are mainly clustered
213 within proteins belonging to the Golgi apparatus and microtubules regulation.

214 For subsequent validation experiments, we decided to focus on protein activators of ASOs since
215 we were more interested in the mechanistic uptake and trafficking of ASOs in cells. From the
216 list of activators having 3 effective sgRNAs we highlighted COG8 and Rab5C, two known and
217 well characterized positive regulators of PS-ASOs productive trafficking and activity in
218 different cell lines.[35,36] This finding further supports the validation and robustness of our
219 screening experiment. As a first set of genes, we selected Elmo Domain Containing 1
220 (ELMOD1), Fumarate Hydratase (FH), Transcriptional Adapter 2-Beta (TADA2B) and
221 Williams-Beuren Syndrome Chromosome Region 16 (WBSCR16), which are from to the top
222 ranked candidates with 4 sgRNAs fulfilling the chosen criteria. We also selected WDR91 as it
223 is an important factor that participates in the negative regulation of phosphatidylinositol–3–
224 phosphate (PtdIns3P) allowing the early-to-late endosome conversion.[45,46] This first pool of 5
225 genes was considered as a nonbiased sampling of potential activator candidates to be further
226 investigated.

227

228 **WDR91 promotes tcT3- and LNA T3-ASOs activity in 501Mel cells**

229 An RNA interference experiment was designed to further validate the five selected candidates
230 as ASO activity enhancers (**Figure 5A**). After protein knockdown, the tcT3 activity should be
231 reduced resulting in increased cell proliferation compared to a control condition.

232 It was already well established in previous *in vitro* studies that the protein ANXA2 was an
233 important facilitator of PS-ASOs endosomal trafficking in various cell lines.[37] We thus first
234 evaluated the effect of ANXA2 downregulation in 501Mel cells proliferation with or without
235 tcT3 in comparison with a control siRNA. A western blot analysis confirmed the
236 downregulation of ANXA2 protein after cells treatment with an ANXA2 siRNA

237 (**Supplemental Figure S3A**). As shown in **Figure 5B**, *ANXA2* mRNA knockdown
238 significantly impaired the activity of tcT3 by comparison with a control siRNA.

239 As for ANXA2, each individual candidate (WBSCR16, TADA2B, FH, ELMOD1 and WDR91)
240 was downregulated with a corresponding siRNA (or a control siRNA) for 48h. The knockdown
241 efficiencies were confirmed by qPCR analysis (**Supplemental Figure S3B** – Apart from
242 ELMOD1, all knockdowns were shown to be significant enough to allow a relevant biological
243 effect). 501Mel cells were then reverse transfected with either the siRNA alone or a
244 combination of siRNA and tcT3. Four days after the second transfection, the cell density was
245 measured by a crystal violet colorimetric assay (**Figure 5A**). After normalizing the cell density
246 to each of the corresponding single siRNA treatment, WDR91 and TADA2B knockdowns
247 showed a significant inhibition of tcT3 anti-proliferative activity (**Figure 5C and Table 2**). In
248 these conditions, WDR91 knockdown cells showed the most significant and reproducible
249 effect. Therefore, we decided to focus on WDR91 in our next investigations.

250 We next wondered whether this mechanism was PS-ASO chemistry dependent and carried out
251 the same experiment as above but with the LNA version of the TSB-T3. Again, in these
252 conditions, ANXA2 and WDR91 knockdowns showed a significant inhibition of the LNA-T3
253 anti-proliferative activity (**Figure 5D and Table 3**), indicating that this mechanism was not PS-
254 ASO chemistry dependent.

255 Melanoma cells proliferation can also be promoted by the level of *TYRP1* mRNA expression.[38]
256 qPCR analysis show that *TYRP1* mRNA expression level is not significantly affected by the
257 transfection of control, ANXA2 or WDR91 siRNAs (**Supplemental Figure S3C**).

258

259

260

261 **WDR91 enhancer activity is PS-ASO sequence dependent**

262 We identified WDR91 in melanoma cells using a fully modified TSB ASO and wondered
263 whether similar effects would hold true in a different system (different mechanism of action
264 and cell line). Indeed, it is known that human cancer cell lines have very heterogenous ASO
265 uptake efficiencies. To address this question, we first transfected the U2OS osteosarcoma cell
266 line with siRNAs (control or directed against ANXA2 or WDR91) and evaluated the effect on
267 LNA GMs activity (mRNA knockdown) directed against Metastasis Associated Lung
268 Adenocarcinoma Transcript 1 (*MALAT1*) and Inhibitor of Growth Family Member 2 (*ING2*)
269 RNAs. From these two RNAs, *MALAT1* is a highly studied and conserved nuclear lncRNA and
270 is abundantly expressed in many cells. The experimental workflow is depicted in **Figure 6A**.
271 RT-qPCR in control-siRNA conditions confirmed the efficient downregulation of *MALAT1* and
272 *ING2* mRNAs by their respective GM (**Figure 6B**). No impact was observed regarding either
273 MALAT1 or ING2 ASO-mediated mRNAs knockdowns after ANXA2 downregulation.

274 We observed that WDR91 knockdown efficiently abrogated MALAT1 ASO activity (**Figure**
275 **6C**), confirming the putative role of this protein in ASO potency. However, no such effect was
276 observed on ING2 ASO activity. Both 16-mers MALAT1 and ING2 GMs have the same design
277 and chemistry and only differ by their respective sequence. Considering that proteins interact
278 with ASOs in a sequence dependent manner,[47] this suggests that WDR91 activity is PS-ASO
279 sequence dependent.

280 Together, these data highlight for the first time, a set of proteins that can modulate PS-ASO
281 potency in a melanoma cell line, and in a physiological context. Among these candidates,
282 WDR91 is a strong regulator. Its activity has been confirmed in two distinct cell lines but could
283 be ASO-sequence dependent.

284

285 **WDR91 does not influence PS-ASOs activity in muscle cells**

286 To evaluate the potency of WDR91 to affect PS-ASOs activity in a different context, we
287 assessed WDR91 ability to influence the activity of a splice-switching ASO used to mediate
288 exon skipping in skeletal muscle cells. ASO-mediated exon-skipping is indeed one of the most
289 promising therapeutic approaches for the treatment of Duchenne muscular dystrophy (DMD).
290 The mechanism of action of ASO in this context is to mask important regulatory splicing signals
291 to exclude the targeted exon and restore the reading frame of the DMD pre-mRNA.[48]
292 Immortalized human myoblasts from DMD patients are typically used as a model to study
293 dystrophin restoration mediated by splice switching oligonucleotides (SSOs). Here we used
294 immortalized DMD myoblasts carrying a deletion of DMD exon 52 leading to an out-of-frame
295 mRNA and resulting in the absence of dystrophin. The use of an SSO directed against the exon
296 51 (SSOEx51) allows to restore the open-reading frame of the dystrophin mRNA.

297 To study the effect of WDR91 on SSOEx51 activity, the immortalized KM571 cells were first
298 transfected with siRNAs to knockdown WDR91 or ANXA2 expression (**Figure 7A**). Seventy-
299 two hours later cells were treated with the SSOEx51 (LNA/2'OMe PS mixmer) to study exon
300 51 skipping efficiency in a context where WDR91 or ANXA2 expression was reduced. RNA
301 was extracted to first check knockdown efficiency, and we confirmed that siRNAs treatment
302 resulted in a strong knockdown (>70 %) of *WDR91* and *ANXA2* respective mRNAs (**Figure**
303 **7B**). Exon skipping levels were then compared and normalized to the siRNA control group
304 (siCTL). We noted a significant reduction in the exon skipping efficacy when ANXA2
305 expression was reduced (**Figure 7C**). However, this effect was not observed with WDR91.
306 Similar results were obtained with a different SSO chemistry (2MOE PS) (**Supplemental**
307 **Figure S4**), indicating that WDR91 is not a modulator of PS-ASOs in this system.

308 To determine whether this effect was specific to SSOs or to KM571 cells, we used a different
309 type of ASO to clarify the role of WDR91 in these cells. As described above, we first transfected
310 the KM571 cells with siRNAs targeting *WDR91* or *ANXA2* mRNAs and then with a GM against
311 *MALAT1* mRNA (GM MALAT1) (**Figure 7D**). Here again, siRNA-induced knockdown of
312 *WDR91* and *ANXA2* was very efficient (**Figure 7E**). When quantifying the levels of *MALAT1*
313 mRNA, we observed no significant differences between the siRNA treatment (control, ANXA2
314 or WDR91) (**Figure 7F**) indicating that WDR91 or ANXA2 knockdown did not affect GM
315 MALAT1 activity. These results suggest that WDR91 likely does not contribute to PS-ASO
316 activity in KM571 cells, regardless of the type of PS-ASOs used.

317

318

319

320

321

322

323

324

325

326

327

328

329

330 **DISCUSSION**

331 Despite many clinical successes, the precise mechanisms of ASOs uptake and trafficking
332 remain to be fully understood. In this study, we used a genome-wide CRISPR inhibition screen
333 to identify without *a priori* proteins involved in PS-ASO trafficking, release and productive
334 activity in a 501Mel cell line. Our CRISPR knockout screening strategy has enabled us to
335 discover functionally involved proteins, using a 3rd generation ASO and preserving the integrity
336 of intracellular membranes and organelles. Moreover, the miRNA displacement mediated by a
337 Target Site Blocker ASO represents a relevant assay to investigate the proteins involved in
338 ASOs efficiency and which has been validated *in vivo*.

339 This study revealed a set of 95 potential activators and 55 inhibitors. Among the activators, our
340 assay highlighted the Rab5C and COG8 proteins, which are known positive regulators of ASOs
341 trafficking and productive activity.[35,36] ANXA2, which is another known positive regulator,
342 was not found in the list of candidates after application of our filters, which also shows that this
343 type of CRISPR screen can be subject to false negatives.

344 In this study, we focused on WDR91 protein as a candidate of interest. This protein has a strong
345 biological relevance as it is known to participate in the early-to-late endosome conversion and
346 its knockdown showed the most significant inhibition of tcT3 anti-proliferative activity in our
347 validation experiments.

348 We confirmed that WDR91 was a positive modulator of PS-ASO activity in two different
349 assays (cell density assay and mRNA knockdown performance), with different cell models
350 (501Mel and U2OS) and ASO chemistries (tcDNA TSB and LNA GM), a landmark result of
351 this project. The impact of WDR91 was not validated in all the systems studied. Indeed,
352 although our results are similar when comparing the ASO activity of WDR91 in 501Mel and
353 U2OS cells, they tend towards an ASO sequence-related activity. In addition, WDR91 did not

354 have any effect with a splice-switching ASO in muscle cells. Thus, as is the case for ANXA2,
355 WDR91 may have an ASO-promoting activity that is also cell line-dependent. Indeed, it is
356 known that identified proteins involved in ASO trafficking and productive activity might not
357 have the same impact depending on the cell line (probably due to differences in high isoform
358 co-expression or the establishment of compensatory proteins or pathways). The same
359 observation was made, for example, in a study evaluating Rab5C, a well-characterized
360 modulator of ASO activity.[49]

361 Ultimately, the results of our validation experiments on various cell systems and ASO
362 chemistries underline the need for caution when identifying an ASO modulator in a specific
363 context, as it may not be applicable to all systems.

364 Interestingly, other studies have highlighted WDR91 as an important mediator of the release
365 and efficacy of internalized reoviruses or antibody-drug conjugates in cells during the early
366 endosome maturation or from the late endosomes.[50,32] Therefore, this study tends to further
367 reinforce the key role of endosomal proteins in productive ASO trafficking and activity.

368 One of the limitations of our study is that genome-wide CRISPR screening was performed in a
369 single replicate. Rigorous filters were used to identify robust ASO activity modulators. We
370 have chosen to focus on a few selected proteins that promote internalized ASO activity, but it
371 would also be interesting to validate other identified proteins as well as the potential inhibitors
372 to confirm other candidates in 501Mel cells, as well as in other melanoma cell lines with
373 different states of cell differentiation. Furthermore, and given the specificity of this cell type
374 with regard to melanosome biogenesis and transport, involving numerous traffic processes,[51] it
375 would be of interest to further evaluate WDR91 in other cell lines as it has been done in U2OS
376 and KM571 cells.

377 Analysis of the gene set enrichment also suggested new avenues to explore. Looking at the
378 inhibitory proteins, some of them were associated with the endosomal cellular compartment.
379 ATP6V0D2, for example, is one of the strongest inhibitor candidates in our selection and is
380 involved in the acidification and pH maintenance in certain intracellular compartments.[52] Some
381 activator candidates might be related to actin cytoskeleton regulation. From the related proteins,
382 CDC42 and MAP2 are known to be involved in cellular trafficking disorders.[53] It is therefore
383 relevant to consider that a defect in these proteins could also have an impact on intracellular
384 trafficking and ASO release in melanoma.

385 Ultimately, our results contribute to a better characterization and identification of protein
386 modulators of ASO activity, providing valuable information for potential new therapeutic
387 avenue. Potent ASO modulators validated *in vitro* could be inhibited or overexpressed in *in*
388 *vivo* experiments to assess and confirm an increase in ASO potency. Acting at the level of these
389 modulators or directly on ASO-modulators interaction could result in more productive ASO
390 activity, triggering an exacerbated inhibitory effect and an overall increase in the therapeutic
391 index.

392

393

394

395

396

397

398

399

400 **MATERIALS AND METHODS**

401 **Cell lines and lentiviral library**

402 501Mel and U2OS cells were acquired from ATCC. Before experiments, all cells were
403 regularly tested for absence of mycoplasma. Culture and sub-culturing were performed in
404 RPMI-1640 (Gibco) for 501Mel and Mc Coy's 5A (Gibco) for U2OS, supplemented with 10%
405 fetal bovine serum (FBS) (Gibco), 2mM L-glutamine (Gibco) and 1% penicillin/streptomycin,
406 (Gibco) and cultured at 37°C in a humidified incubator with 5% CO_2. Transfections and
407 infections were performed in the same media but without antibiotics and with a
408 decomplemented serum (30 minutes at 56°C). Immortalised myoblasts carrying a deletion of
409 DMD exon 52 (KM571) were obtained from the platform for immortalization of human cells
410 from the Institut de Myologie. KM571 cells were grown in a 50/50 mix of skeletal muscle cell
411 growth medium (Promocell, Germany) and F-10 (Thermo Fisher Scientific, USA) with 10%
412 fetal bovine serum, and 1% penicillin-streptomycin (100 U/mL).

413

414 **Antisense oligonucleotides**

415 miRCURY LNA™ Target site blockers TSB-C1 (ACTTTATTACAATCAT) and TSB-T3
416 (ACACAGTGGCAAACAC) were designed and obtained from Qiagen. tcC1 and tcT3 were
417 synthesized from SQY Therapeutics (Montigny le Bretonneux) as fully modified tcDNA-PS
418 ASOs. The TSB-C1 and tcC1 controls have no significant match to any annotated human
419 3'UTR. MALAT1 (CGTTAACTAGGCTTTA) and ING2 (TACGTTGGCTTGTTCA) LNA
420 Gapmers were designed and obtained from Qiagen. For the KM571 experiments, all ASOs were
421 obtained from Eurogentec. Two chemistries of the splice switching oligonucleotide targeting
422 exon 51 (SSOEx51 previously described)[54] were used: LNA/2'OMe PS mixmer and full 2MOE

423 PS. MALAT1 GM is a 2MOE PS (previously described).[37] All ASOs were reconstituted in
424 nuclease-free water (Invitrogen).

425

426 **siRNAs**

427 siRNAs pools were purchased from Santa Cruz (Negative Control A sc-37007; WDR91 sc-
428 89398; WBSCR16 sc-89899; FH sc-105377; ELMOD1 sc-77261; TADA2B sc-156169;
429 ANXA2 sc-270151)

430

431 **Generation of 501Mel knockout library**

432 Transduction of mycoplasma negative 501Mel cells at 60% confluence was performed in T175
433 flasks (standard - Sarstedt) with the Brunello knockout pooled lentiviral library from Addgene
434 (# 73179-LV) and in RPMI-1640 decomplemented medium (Gibco) without antibiotics. The
435 Brunello pooled lentiviral library contains 76,441 single guides RNAs (sgRNAs), targeting
436 19,114 coding genes (4 sgRNAs per gene). A multiplicity of infection (MOI) of 0.4 was
437 selected to ensure that every single cell is infected with only one sgRNA. Twenty-four hours
438 later, the infectious medium was replaced by a fresh complete medium. After 48h, infected cells
439 were positively selected with 2.5µg/mL puromycin (InvivoGen) for 7 days. Following selection
440 and expansion of the surviving cells, around 350 million cells were recovered. A dry pellet of
441 100 million cells was prepared for gDNA extraction and sequencing. The remaining cells were
442 used for the subsequent reverse transfection.

443

444

445

446 **RNA interference, ASO treatments and cell density assay**

447 **501Mel parental cells.** Reverse-transfections of siRNAs were performed in 60mm dishes
448 (standard - Sarstedt) with 224,000 cells per dish and for 48h in RPMI-1640 decomplemented
449 medium without antibiotics. Briefly, 1mL lipoplexes layers were formed with Lipofectamine
450 2000 (Invitrogen) and the siRNA concentrations were set to 30nM in a final 3mL volume after
451 addition of the cells on top of the lipoplexes. For all the transfections, lipoplexes were formed
452 in OptiMEM®. After 16h incubation, the medium was replaced by a fresh complete medium
453 without antibiotics. After 48h, the cells were recovered, counted with a Neubauer counting
454 chamber and a second reverse-transfection was performed in 96-well plates (standard F-
455 Sarstedt) with 3000 cells per well and with either the siRNA alone (at 30nM final concentration)
456 or a combination of siRNA (30nM) and tcT3 or LNA T3 at a final concentration of 50nM in a
457 final volume of 150µL (100µL of cells on top of 50µL of lipoplexes). After 16h incubation, the
458 medium was replaced by a fresh 150µL complete medium without antibiotics. After 4 days
459 following to the second transfection, the cell density was measured with 0.5% crystal violet (10
460 minutes at RT, followed by three PBS washes, 100µL of 100% EtOH solubilization and
461 absorbance reading at 590nm using a Tecan Infinite F200 Pro reader).

462 **U2OS cells.** Reverse-transfections of siRNAs were performed in 12-well plates (standard -
463 Sarstedt) with 50,000 cells per well and for 48h in decomplemented Mc Coy's 5A medium
464 without antibiotics. Cell density was optimized so these cells are efficiently transfected between
465 20 and 30% confluence. The procedure was the same as described above except that the siRNA
466 transfection was performed with RNAiMax (Invitrogen) and 6h post seeding. After 48h, the
467 medium was replaced by 0.4mL of a fresh decomplemented Mc Coy's 5A medium without
468 antibiotics and a reverse-transfection with Lipofectamine 2000 was performed in the same plate
469 with the MALAT1 or ING2 Gapmer (at 30nM final concentration) in a final volume of 0.8mL

470 (0.4mL of lipoplexes on top of the cells). After 24h following to the second transfection, total
471 RNA was extracted for further RT-qPCR analysis.

472 **501Mel knockout library.** Reverse-transfections of tcT3 and C1 were performed in 150mm
473 dishes (standard - Sarstedt) with 1.5 million knockout cells per dish and for 72h in RPMI-1640
474 decomplemented medium without antibiotics. Briefly, 10mL lipoplexes layers were formed
475 with Lipofectamine 2000 (Invitrogen) and the respective ASOs concentrations were set to
476 50nM in a final 24mL volume after addition of the cells on top of the lipoplexes. For the
477 transfections, lipoplexes were formed in OptiMEM® and the mycoplasma-negative knockout
478 cells have been sub-cultured 24h before in T175 flasks (standard - Sarstedt). The cells
479 confluency at the day of transfection was maintained between 50 and 80%. After 7h of
480 transfection, the medium was replaced by a fresh complete medium without antibiotics. To
481 ensure a coverage of 400 cells per guide RNA in our library, a total of 32 million cells was
482 transfected with either the tcT3 or C1. Thus, 22 dishes were used per oligonucleotide
483 transfection. After 72h of transfection, surviving cells were recovered and pellets of 100 million
484 cells were kept at -80°C until further processing.

485 **KM571 cells.** Cells were plated in 6-well plates (300,000 cells per well) and transfected the
486 same day with 20nM of siRNA with Lipofectamine RNAiMAX according to the
487 manufacturer's instructions (Thermo Fisher Scientific, USA). Twenty-four hours after the first
488 transfection, proliferation medium was changed for differentiation medium (DMEM, 2% horse
489 serum, 1% penicillin / streptomycin (100 U/mL)) to induce myotubes formation. After 3 days
490 of differentiation, cells were treated with 100nM of the SSOEx51 for 24h with Lipofectamine
491 LTX according to the manufacturer's instructions (Thermo Fisher Scientific, USA). For the
492 transfection of the GM MALAT1, similar protocol was used, except that KM571 cells were
493 only treated during proliferation and that the GM MALAT1 treatment was performed for 48h.

494 **NGS sequencing library preparation**

495 Frozen pellets of 100 million transfected surviving cells (and from non-treated knockout
496 library) in 50mL poplypropylene tubes (Sarstedt) were thawed on ice for 20 minutes and lysed
497 at room temperature. Genomic DNA was purified according to the manufacturer's instructions
498 (NucleoBond HMW DNA, Macherey-Nagel). A total of 280µg of genomic DNAs was used for
499 PCR amplification of sgRNA sequences, using the Herculase II Fusion polymerase (Agilent).
500 Illumina P5- and P7-barcoded adaptors were used, and PCR amplification and quality controls
501 have been carried out as described by Zhang laboratory (Joung *et al*, 2017). Amplified PCR
502 products were purified using AMPure XP beads (Beckman Coulter) according to the
503 manufacturer's instructions, eluted in 14µL of nuclease-free water (Invitrogen) and stored at -
504 20°C until Bioanalyzer quality control (TapeStation 4200, Agilent) was used to measure the
505 size, quality and concentration. The pooled samples were sequenced using Illumina NGS
506 sequencing platform (Novaseq6000 – CurieCoreTech ICGex Platform).

507

508 **NGS data analysis**

509 MAGeCK (v0.5.9.4) was used to extract sgRNA read counts from the samples fastq.gz files
510 (mageck count program with the --norm-method median option). For each sgRNA, we
511 transformed the read counts onto M (log ratio) and A (mean average): M =
512 log2(sgRNA_count_in_TRT+1) - log2(sgRNA_count_in_CTL+1), and A = mean
513 (count_TRT, count_CTL) in log2 scale. Fold-changes between TRT and CTL conditions were
514 also computed from the M values of each sgRNA.

515

516

517 **RNA extraction and RT-qPCR analysis**

518 Total RNA form cell lysates was obtained using a NucleoSpin® RNA kit (Macherey-Nagel),
519 according to the manufacturer's instructions and with on-column DNAse treatment. After
520 Nanodrop evaluation of purity and concentration, 500ng of RNA was used for reverse-
521 transcription (MultiScribe RT – Applied Biosystems). Obtained cDNA was diluted to 2.5ng/µL
522 and used as template for qPCR using a QuantStudio5 system (Applied Biosystems). SYBR
523 Green (PowerSYBR® Green PCR Master Mix – Applied Biosystems) was used according to
524 the manufacturer's instructions. For each sample measurement, 3 technical replicates were
525 performed. TBP was used as internal standard. TYRP1 and ING2 primers were purchased from
526 Eurogentec. % knockdown was calculated as $100*(1-2^{-ddCt})$. Total RNA was isolated from
527 cultured human myoblast cells using TRIzol reagent, according to the manufacturer's
528 instructions (Thermo Fisher Scientific, USA). Aliquots of 1 µg of total RNA were used for RT-
529 PCR analysis. The cDNA synthesis was carried out with LunaScript™ RT SuperMix Kit (New
530 England Biolabs). Exon 51 skipping was measured by TaqMan qRT-PCR, using TaqMan
531 assays that were designed against the exon 51-53 or exon 50-53 templates using the Prime Time
532 qPCR probe assays (Integrated DNA Technology) (Assay Ex51-53 - forward : 5'-
533 CAGGTTGTGTCACCAGAGTAA-3'; reverse 5'-TGAGTGGAAGGCGGTAAA-3'; probe :
534 5'-/56-FAM/TGACCACTA/ZEN/TTGGAGCCTCTCCTAC/3IABkFQ/-3' and assay Ex50-
535 53: forward: 5'-ACTGATTCTGAATTCTTTCAAAGGC-3'; reverse: 5'-
536 TTCAAGAGCTGAGGGCAAAG-3'; probe: 5'- /56-
537 FAM/ACCTAGCTC/ZEN/CTGGACTGACCACT/3IABkFQ/-3') . gBlocks Gene Fragments
538 (Integrated DNA Technology) from human exon 49-54 and human exon 49-54 Delta 52 were
539 used as standards for DNA copy number. 70 ng of cDNA was used as input per reaction, and
540 all assays were carried out in triplicate. Assays were performed under fast cycling conditions
541 on a Bio-Rad CFX384 Touch Real-Time PCR Detection System. For a given sample, the copy

542 number of skipped product (exon 50-53 assay) and unskipped product (exon 51-53 assay) was
543 determined using the standards Ex49-54 and Ex49-54 Delta52, respectively. Exon 51 skipping
544 was then expressed as a percentage of total dystrophin. Knockdown analysis was performed by
545 using the appropriate probes for the studied targets and were purchased from Integrated DNA
546 technologies (IDT) (MALAT1 Hs.PT.58.26451167.g; WDR91 Hs.PT.58.39523053 and
547 ANXA2 Hs.PT.56a.40676274). The expression of the different targets was then normalized to
548 a reference gene (GAPDH Hs.PT.39a.22214836).

549

550 **Protein isolation and Western blotting**

551 Total protein extracts were obtained by resuspension of PBS-washed cell pellets in 40µL of
552 ice-cold RIPA buffer (Tris-HCl 50 mM, ph7.4, NaCl 150 mM, Sodium Deoxycholate 0.5%,
553 Triton 1%, SDS 0.1%), including protease inhibitor cocktail (Sigma-Aldrich, P8340) and
554 centrifugation at 16,000xg for 15min at 4°C. Proteins quantification from the cleared lysates
555 was performed using a Pierce™ BCA Assay kit (Thermo scientific). After 4-12% SDS-PAGE
556 in NuPAGE MES buffer (Invitrogen), proteins were transferred onto PVDF membranes with a
557 turbo transfer system (BIO-RAD) for 10 minutes at 25V and 2.5A. After transfer, the
558 membranes were washed in Tris-buffered saline and 0.1% Tween 20 (TBST) and blocked for
559 30 minutes at room temperature in a solution of TBST + 5% w/v non-fat dry milk. Blocked
560 membranes were washed three times in TBST for 5 minutes and diluted primary antibody was
561 incubated at 4°C overnight with shaking. The diluted HRP-conjugated secondary antibody was
562 added for 1h at room temperature with shaking, after three TBST washes of 5 minutes. Imaging
563 was performed after ECL reagent addition and chemiluminescence detection with G:Box
564 Chemi XX6 imager from Syngene. ANXA2 antibody was purchased from Santa Cruz (sc-
565 28385).

566 **Statistical analysis**

567 GraphPad Prism software (San Diego, CA, USA) version 9.5.1 was used for statistical analysis
568 and graphs design. Each data is presented as mean of at least three independent biological
569 replicates with standard deviation (SD). P-values were calculated by two-sided unpaired *t*-tests
570 with Welch's correction and differences were statistically significant at $*p \leq 0.05$; $**p \leq 0.01$;
571 $***p \leq 0.001$; $****p \leq 0.0001$. For exon skipping experiments, normal distribution of samples
572 was assessed by using Shapiro-Wilk test. Comparisons of statistical significance were assessed
573 by one-way ANOVA parametric test or Kruskal-Wallis non-parametric test and followed by
574 appropriate post-hoc tests if applicable.

575

576 **DATA AVAILABILITY STATEMENT**

577 Data are available upon request to the corresponding author.

578

579 **ACKNOWLEDGMENTS**

580 The authors thank the SFR Biosit L3 platform of Rennes University for providing the required
581 facility for performing the lentiviral infections. The authors also thank the Institut Curie
582 (Genetic screen CRISPR'it and ICGex Core Facilities) for performing the NGS sequencing,
583 SQY Therapeutics for providing the tcDNA-ASO molecules and the platform for the
584 immortalization of human cells from the Institut de Myologie for the human-derived cells. This
585 study received financial support from the Agence Nationale de la Recherche (ANR).

586

587

588 **AUTHOR CONTRIBUTIONS**

589 G.M., R.P., D.G., A.Go. and A.Ga. conceived and analyzed the experiments. G.M. and A.Ga.
590 performed the experiments. M.A. analyzed the NGS raw data. A.M. and A.B. helped in the
591 library preparation. G.M. wrote the manuscript. All the authors reviewed the manuscript.

592

593 **DECLARATION OF INTERESTS**

594 The authors declare no competing financial interests.

595

596 **KEYWORDS**

597 CRISPR screen; NGS; Antisense Oligonucleotides (ASOs); Melanoma; Target Site Blockers
598 (TSBs); protein modulators of ASOs; endosomes; productive activity; WDR91.

599

600 **REFERENCES**

601 [1] Stanley T. Crooke et al., "Antisense Technology: A Review," *The Journal of Biological Chemistry* 296
602 (February 16, 2021): 100416, https://doi.org/10.1016/j.jbc.2021.100416.

603 [2] J. Kim et al., "Patient-Customized Oligonucleotide Therapy for a Rare Genetic Disease," *The New England*
604 *Journal of Medicine* 381, no. 17 (October 24, 2019): 1644–52, https://doi.org/10.1056/NEJMoa1813279.

605 [3] Stanley T Crooke et al., "Cellular Uptake and Trafficking of Antisense Oligonucleotides," *Nature*
606 *Biotechnology* 35, no. 3 (March 1, 2017): 230–37, https://doi.org/10.1038/nbt.3779.

607 [4] Xin Xie et al., "Recent Advances in Targeting the 'Undruggable' Proteins: From Drug Discovery to Clinical
608 Trials," *Signal Transduction and Targeted Therapy* 8, no. 1 (September 6, 2023): 1–71,
609 https://doi.org/10.1038/s41392-023-01589-z.

610 [5] Martin Egli and Muthiah Manoharan, "Chemistry, Structure and Function of Approved Oligonucleotide
611 Therapeutics," *Nucleic Acids Research* 51, no. 6 (March 7, 2023): 2529–73,
612 https://doi.org/10.1093/nar/gkad067.

613 [6] Tina Nie, "Eplontersen: First Approval," *Drugs*, February 28, 2024, https://doi.org/10.1007/s40265-024-
614 02008-5.

[7] Haoyu Xiong, Rakesh N. Veedu, and Sarah D. Diermeier, "Recent Advances in Oligonucleotide Therapeutics in Oncology," *International Journal of Molecular Sciences* 22, no. 7 (March 24, 2021): 3295, https://doi.org/10.3390/ijms22073295.

[8] Maria Gagliardi and Ana Tari Ashizawa, "The Challenges and Strategies of Antisense Oligonucleotide Drug Delivery," *Biomedicines* 9, no. 4 (April 16, 2021): 433, https://doi.org/10.3390/biomedicines9040433.

[9] Suzan M Hammond et al., "Delivery of Oligonucleotide-based Therapeutics: Challenges and Opportunities," *EMBO Molecular Medicine* 13, no. 4 (April 9, 2021): e13243, https://doi.org/10.15252/emmm.202013243.

[10] R.L. Juliano et al., "Cellular Uptake and Intracellular Trafficking of Oligonucleotides: Implications for Oligonucleotide Pharmacology," *Nucleic Acid Therapeutics* 24, no. 2 (April 1, 2014): 101–13, https://doi.org/10.1089/nat.2013.0463.

[11] Alexander Klipp, Michael Burger, and Jean-Christophe Leroux, "Get out or Die Trying: Peptide- and Protein-Based Endosomal Escape of RNA Therapeutics," *Advanced Drug Delivery Reviews* 200 (September 1, 2023): 115047, https://doi.org/10.1016/j.addr.2023.115047.

[12] Steven F. Dowdy et al., "Delivery of RNA Therapeutics: The Great Endosomal Escape!," *Nucleic Acid Therapeutics* 32, no. 5 (October 1, 2022): 361–68, https://doi.org/10.1089/nat.2022.0004.

[13] Philippine Aupy et al., "The Use of Tricyclo-DNA Oligomers for the Treatment of Genetic Disorders," *Biomedicines* 6, no. 1 (December 22, 2017): 2, https://doi.org/10.3390/biomedicines6010002.

[14] "Delivery Is Key: Lessons Learnt from Developing Splice-switching Antisense Therapies | EMBO Molecular Medicine," accessed March 27, 2024, https://www.embopress.org/doi/full/10.15252/emmm.201607199.

[15] Feryal Alhamadani et al., "Adverse Drug Reactions and Toxicity of the Food and Drug Administration-Approved Antisense Oligonucleotide Drugs," *Drug Metabolism and Disposition: The Biological Fate of Chemicals* 50, no. 6 (June 2022): 879–87, https://doi.org/10.1124/dmd.121.000418.

[16] Xue-hai Liang et al., "Identification and Characterization of Intracellular Proteins That Bind Oligonucleotides with Phosphorothioate Linkages," *Nucleic Acids Research* 43, no. 5 (March 11, 2015): 2927–45, https://doi.org/10.1093/nar/gkv143.

[17] Stanley T. Crooke et al., "The Interaction of Phosphorothioate-Containing RNA Targeted Drugs with Proteins Is a Critical Determinant of the Therapeutic Effects of These Agents," *Journal of the American Chemical Society* 142, no. 35 (September 2, 2020): 14754–71, https://doi.org/10.1021/jacs.0c04928.

[18] Xue-Hai Liang et al., "Hsp90 Protein Interacts with Phosphorothioate Oligonucleotides Containing Hydrophobic 2′-Modifications and Enhances Antisense Activity," *Nucleic Acids Research* 44, no. 8 (May 5, 2016): 3892–3907, https://doi.org/10.1093/nar/gkw144.

[19] Colton M. Miller et al., "Stabilin-1 and Stabilin-2 Are Specific Receptors for the Cellular Internalization of Phosphorothioate-Modified Antisense Oligonucleotides (ASOs) in the Liver," *Nucleic Acids Research* 44, no. 6 (April 7, 2016): 2782–94, https://doi.org/10.1093/nar/gkw112.

[20] Thijs Van de Vyver, Stefaan C. De Smedt, and Koen Raemdonck, "Modulating Intracellular Pathways to Improve Non-Viral Delivery of RNA Therapeutics," *Advanced Drug Delivery Reviews* 181 (February 1, 2022): 114041, https://doi.org/10.1016/j.addr.2021.114041.

[21] Brendan T Finicle et al., "Simultaneous Inhibition of Endocytic Recycling and Lysosomal Fusion Sensitizes Cells and Tissues to Oligonucleotide Therapeutics," *Nucleic Acids Research* 51, no. 4 (February 28, 2023): 1583–99, https://doi.org/10.1093/nar/gkad023.

[22]Alexander N. Kapustin et al., "Antisense Oligonucleotide Activity in Tumour Cells Is Influenced by Intracellular LBPA Distribution and Extracellular Vesicle Recycling," *Communications Biology* 4 (November 1, 2021): 1241, https://doi.org/10.1038/s42003-021-02772-0.

[23] Timothy R. Wagenaar et al., "Identification of the Endosomal Sorting Complex Required for Transport-I (ESCRT-I) as an Important Modulator of Anti-miR Uptake by Cancer Cells," *Nucleic Acids Research* 43, no. 2 (January 30, 2015): 1204–15, https://doi.org/10.1093/nar/gku1367.

[24] Shiyu Wang et al., "Membrane Destabilization Induced by Lipid Species Increases Activity of Phosphorothioate-Antisense Oligonucleotides," *Molecular Therapy - Nucleic Acids* 13 (December 2018): 686–98, https://doi.org/10.1016/j.omtn.2018.10.011.

[25] Peter Lorenz et al., "Nucleocytoplasmic Shuttling: A Novel in Vivo Property of Antisense Phosphorothioate Oligodeoxynucleotides," *Nucleic Acids Research* 28, no. 2 (January 15, 2000): 582–92.

[26] "A Stress-Induced Response Complex (SIRC) Shuttles miRNAs, siRNAs, and Oligonucleotides to the Nucleus," accessed March 27, 2024, https://www.pnas.org/doi/epdf/10.1073/pnas.1721346115.

[27] Crooke et al., "The Interaction of Phosphorothioate-Containing RNA Targeted Drugs with Proteins Is a Critical Determinant of the Therapeutic Effects of These Agents."

[28] Liang et al., "Identification and Characterization of Intracellular Proteins That Bind Oligonucleotides with Phosphorothioate Linkages."

[29] Alfred Hanswillemenke et al., "Profiling the Interactome of Oligonucleotide Drugs by Proximity Biotinylation," *Nature Chemical Biology*, January 17, 2024, https://doi.org/10.1038/s41589-023-01530-z.

[30] Christoph Bock et al., "High-Content CRISPR Screening," *Nature Reviews Methods Primers* 2, no. 1 (February 10, 2022): 1–23, https://doi.org/10.1038/s43586-021-00093-4.

[31] Olivier Petitjean et al., "Genome-Wide CRISPR-Cas9 Screen Reveals the Importance of the Heparan Sulfate Pathway and the Conserved Oligomeric Golgi Complex for Synthetic Double-Stranded RNA Uptake and Sindbis Virus Infection," *mSphere* 5, no. 6 (November 11, 2020): e00914-20, https://doi.org/10.1128/mSphere.00914-20.

[32] C. Kimberly Tsui et al., "CRISPR-Cas9 Screens Identify Regulators of Antibody–Drug Conjugate Toxicity," *Nature Chemical Biology* 15, no. 10 (October 2019): 949–58, https://doi.org/10.1038/s41589-019-0342-2.

[33] Douglas Ross-Thriepland et al., "Arrayed CRISPR Screening Identifies Novel Targets That Enhance the Productive Delivery of mRNA by MC3-Based Lipid Nanoparticles," *SLAS Discovery* 25, no. 6 (July 2020): 605–17, https://doi.org/10.1177/2472555220925770.

[34] Moira A. McMahon et al., "GOLGA8 Increases Bulk Antisense Oligonucleotide Uptake and Activity in Mammalian Cells," *Molecular Therapy. Nucleic Acids* 32 (March 27, 2023): 289–301, https://doi.org/10.1016/j.omtn.2023.03.017.

[35] Colton M. Miller et al., "Endosomal Escape of Antisense Oligonucleotides Internalized by Stabilin Receptors Is Regulated by Rab5C and EEA1 During Endosomal Maturation," *Nucleic Acid Therapeutics* 28, no. 2 (April 1, 2018): 86–96, https://doi.org/10.1089/nat.2017.0694.

[36] Petitjean et al., "Genome-Wide CRISPR-Cas9 Screen Reveals the Importance of the Heparan Sulfate Pathway and the Conserved Oligomeric Golgi Complex for Synthetic Double-Stranded RNA Uptake and Sindbis Virus Infection."

[37] Shiyu Wang et al., "Annexin A2 Facilitates Endocytic Trafficking of Antisense Oligonucleotides," *Nucleic Acids Research* 44, no. 15 (September 6, 2016): 7314–30, https://doi.org/10.1093/nar/gkw595.

[38] David Gilot et al., "A Non-Coding Function of TYRP1 mRNA Promotes Melanoma Growth," *Nature Cell Biology* 19, no. 11 (November 2017): 1348–57, https://doi.org/10.1038/ncb3623.

[39] Arthur Gautron et al., "Human TYRP1: Two Functions for a Single Gene?," *Pigment Cell & Melanoma Research* 34, no. 5 (2021): 836–52, https://doi.org/10.1111/pcmr.12951.

[40] Philippine Aupy et al., "Identifying and Avoiding tcDNA-ASO Sequence-Specific Toxicity for the Development of DMD Exon 51 Skipping Therapy," *Molecular Therapy. Nucleic Acids* 19 (November 27, 2019): 371–83, https://doi.org/10.1016/j.omtn.2019.11.020.

[41] "Lowering Mutant Huntingtin Using Tricyclo-DNA Antisense Oligonucleotides As a Therapeutic Approach for Huntington's Disease - PubMed," accessed March 27, 2024, https://pubmed.ncbi.nlm.nih.gov/31184975/.

[42] John G Doench, "Am I Ready for CRISPR? A User's Guide to Genetic Screens," *Nature Reviews Genetics* 19, no. 2 (February 1, 2018): 67–80, https://doi.org/10.1038/nrg.2017.97.

[43] Kendall R. Sanson et al., "Optimized Libraries for CRISPR-Cas9 Genetic Screens with Multiple Modalities," *Nature Communications* 9 (December 21, 2018): 5416, https://doi.org/10.1038/s41467-018-07901-8.

[44] Yanhui Hu et al., "PANGEA: A New Gene Set Enrichment Tool for Drosophila and Common Research Organisms," *bioRxiv*, April 17, 2023, 2023.02.20.529262, https://doi.org/10.1101/2023.02.20.529262.

[45] Kai Liu et al., "WDR91 Is a Rab7 Effector Required for Neuronal Development," *Journal of Cell Biology* 216, no. 10 (October 2, 2017): 3307–21, https://doi.org/10.1083/jcb.201705151.

[46] Nan Liu, Kai Liu, and Chonglin Yang, "WDR91 Specifies the Endosomal Retrieval Subdomain for Retromer-Dependent Recycling," *The Journal of Cell Biology* 221, no. 12 (December 12, 2022), https://doi.org/10.1083/jcb.202203013.

[47] Timothy A. Vickers and Stanley T. Crooke, "Development of a Quantitative BRET Affinity Assay for Nucleic Acid-Protein Interactions," *PloS One* 11, no. 8 (2016): e0161930, https://doi.org/10.1371/journal.pone.0161930.

[48] Aurélie Goyenvalle et al., "Functional Correction in Mouse Models of Muscular Dystrophy Using Exon-Skipping Tricyclo-DNA Oligomers," *Nature Medicine* 21, no. 3 (March 2015): 270–75, https://doi.org/10.1038/nm.3765.

[49] Emily Linnane et al., "Differential Uptake, Kinetics and Mechanisms of Intracellular Trafficking of next-Generation Antisense Oligonucleotides across Human Cancer Cell Lines," *Nucleic Acids Research* 47, no. 9 (May 21, 2019): 4375–92, https://doi.org/10.1093/nar/gkz214.

[50] Anthony J. Snyder, Andrew T. Abad, and Pranav Danthi, "A CRISPR-Cas9 Screen Reveals a Role for WD Repeat-Containing Protein 81 (WDR81) in the Entry of Late Penetrating Viruses," *PLoS Pathogens* 18, no. 3 (March 2022): e1010398, https://doi.org/10.1371/journal.ppat.1010398.

[51] Mitsunori Fukuda, "Rab GTPases: Key Players in Melanosome Biogenesis, Transport, and Transfer," *Pigment Cell & Melanoma Research* 34, no. 2 (2021): 222–35, https://doi.org/10.1111/pcmr.12931.

[52] Sandra Kissing et al., "Vacuolar ATPase in Phagosome-Lysosome Fusion," *The Journal of Biological Chemistry* 290, no. 22 (May 29, 2015): 14166–80, https://doi.org/10.1074/jbc.M114.628891.

[53] Angeles García-Cazorla et al., "Genetic Disorders of Cellular Trafficking," *Trends in Genetics* 38, no. 7 (July 2022): 724–51, https://doi.org/10.1016/j.tig.2022.02.012.

[54] Amel Saoudi et al., "Investigating the Impact of Delivery Routes for Exon Skipping Therapies in the CNS of DMD Mouse Models," *Cells* 12, no. 6 (January 2023): 908, https://doi.org/10.3390/cells12060908.

738 **FIGURE LEGENDS**

739 **Figure 1. Inhibition of 501Mel cells proliferation with Target Site Blocker ASOs targeting**
740 ***TYRP1* mRNA.** (A) A competition mechanism occurs with binding of TSB-T3 to a sequence
741 overlapping the miR-16 site in the 3'UTR of *TYRP1* mRNA, thus releasing miR-16 whose
742 tumor suppressor activity is restored. TSB-C1 (Control ASO) has no match with *TYRP1*
743 3'UTR.[38] The cell density assay upon TSB-C1 or -T3 treatment is measured through a crystal
744 violet colorimetric assay. The **figure 1A** was generated with BioRender.com (B) 501Mel cell
745 density assay at day 3 with increasing concentrations of reverse-transfected LNA- (T3) or
746 tcDNA- (tcT3). Experiments were performed in independent biological triplicates. Data were
747 normalized to the corresponding control conditions (C1 or tcC1) at the same concentrations
748 (10, 30, 50 and 70nM). Data are presented as mean (SD). Unpaired *t*-test with Welch's
749 correction were performed. The statistical significance is **P=0,0040 (T3 *vs* C1 – 30nM);
750 *P=0,0241 (T3 *vs* C1 – 50nM); **P=0,0061 (T3 *vs* C1 – 70nM); **P=0,0078 (tcT3 *vs* tcC1 –
751 30nM); **P=0,0036 (tcT3 *vs* tcC1 – 50nM); *P=0,0105 (tcT3 *vs* tcC1 – 70nM).

752

753 **Figure 2. Generation and treatment of the 501Mel cells knockout library.** (A) Workflow
754 of the experimental setup. S1: Step 1 (cells transduction – non infected cells in grey on the
755 workflow); S2: Step 2 (transduced cells positive selection with antibiotic); S3: Step 3 (ASO
756 exposure); S4: Step 4 (gDNA purification and sgRNAs amplification). The figure was
757 generated with BioRender.com (B) Distribution of the number of normalized read counts per
758 sgRNA in the tcT3 and the tcC1-treated library. The mean is represented by a red bar (C)
759 Method for identifying genes promoting or inhibiting ASO uptake and/or efficiency after NGS
760 sequencing and based on normalized read counts after tcC1 or tcT3 treatment.

761

762 **Figure 3. NGS sequencing data sorting and analysis.** (A) After sgRNA extraction, MA plots
763 are used to visualize the differences between measurements (read counts) between two
764 conditions: treatment (tcT3) *versus* control (tcC1). For each sgRNA, the read counts are
765 transformed onto M (log ratio) and A (mean average) scales. M is equal to
766 log2(sgRNA_count_in_TRT+1) - log2(sgRNA_count_in_CTL+1) and A is the mean between
767 count_TRT and count_CTL in log2 scale. Candidates' selection was performed according to
768 the following criteria: A ≥ 6 and M ≥ 0.6 (enriched sgRNAs, ASOs activators); A ≥ 6 and M ≤
769 -0.6 (depleted sgRNAs, ASOs inhibitors). Control sgRNAs (non-targeting guides) are located
770 between M ≥ 0.6 and M ≤ -0.6. On the obtained MA plot, red, green and black dots represent
771 the genes with the 4, 3 and 2 sgRNAs over 4 fulfilling the defined criteria, respectively (B) MA
772 plot examples from selected activator and inhibitor candidates with applied M and A filters and
773 with 4 (GGTLC2) or 2 relevant sgRNAs (WDR91). The yellow dots represent the genes with
774 a very low expression in either the treatment or the control condition and as a consequence, an
775 elevated but non-significant fold change (C) Representation of the post-sequencing normalized
776 read counts in the control (CTL – tcC1) and treated (TRT – tcT3) conditions for the sgRNAs
777 of four sorted modulator candidates (COG8, WBSCR16, WDR91, in red – activators; GGTLC2
778 in blue – inhibitor). The fold change is calculated as: tcT3 read counts / tcC1 read counts (for
779 activators); tcC1 read counts / tcT3 read counts (for inhibitors).

780

781 **Figure 4. ASO activators and inhibitors ranking and selection.** (A) Distribution of the
782 average fold change (tcT3 read counts *vs* tcC1 read counts) from the fold changes of the 2, 3 or
783 4 corresponding sgRNAs per gene, for 53 of the 95 selected ASO activator candidates (fulfilling
784 the criteria A ≥ 6 and M ≥ 0.6 on the MA plot). Green stars represent candidates that have
785 already characterized in the literature. Black stars correspond to the 5 candidates that have been
786 chosen for further functional validation (B) Distribution of the average fold change (tcC1 read

787 counts *vs* tcT3 read counts) from the fold changes of the 2, 3 or 4 corresponding sgRNAs per
788 gene, for 31 of the 55 selected ASO inhibitor candidates (fulfilling the criteria A ≥ 6 and M ≤ -
789 0.6 on the MA plot). The fold change threshold was fixed to 1.5. The full list activator and
790 inhibitor candidates is provided in **Table 1**.

791

792 **Figure 5. Functional validation of tcT3 activity enhancer candidates in 501Mel cells.** (A)
793 Workflow of the experimental design (B) Setup of the 501Mel cell density assay with ANXA2
794 positive control. Cell density measurement was performed by crystal violet assay after tcT3
795 transfection on normal, control or ANXA2 knockdown cells (NT: Non-Treated; siCTL: control
796 siRNA). The relative cell density in each condition is normalized to the non-treated cells. (C)
797 501Mel cell density assay after tcT3 transfection on normal, control or candidate's knockdown
798 cells. Data are represented with a cell density normalized to 100% for each treatment with the
799 siRNA alone, to discard any proliferation bias induced by the siRNA's effects. (D) 501Mel cell
800 density assay after LNA T3 transfection on normal, control, WDR91 or ANXA2 knockdown
801 cells. Data are represented with a cell density normalized to 100% for each treatment with the
802 siRNA alone, to discard any proliferation bias induced by the siRNA's effects. Experiments
803 were performed in independent biological replicates. Data are presented as mean (SD).
804 Unpaired *t*-test with Welch's correction were performed. The statistical significance is Panel
805 C: *P=0,0468 (TADA2B, N=3); **P=0,0011 (WDR91, N=4); ****P≤0,0001 (ANXA2, N=5);
806 NS= non-significant (P=0,0588); Panel D: *P=0,0154 (WDR91, N=5); ***P=0,0004 (ANXA2,
807 N=5).

808

809 **Figure 6. Functional validation of WDR91 in U2OS cells.** (A) Workflow of the experimental
810 design (B) *MALAT1* and *ING2* mRNA quantification by RT-qPCR at D4 and D5 respectively,

811 after corresponding GM transfection on non-treated, control or ANXA2 knockdown cells. The
812 relative mRNA fold change was normalized to the non-treated condition (no siRNA
813 transfection). Experiments were performed in independent biological triplicates (MALAT1)
814 and quadruplicates (ING2). Data are presented as mean (SD). Unpaired *t*-test with Welch's
815 correction were performed. The statistical significance is **P=0,0019 (NT *vs* siCTL);
816 ****P<0,0001 (NT *vs* siCTL; NT *vs* siANXA2) (C) *MALAT1* and *ING2* mRNA quantification
817 by RT-qPCR at D4 and D5 respectively, after corresponding GM transfection on non-treated,
818 control or WDR91 knockdown cells. The relative mRNA fold change was normalized to the
819 non-treated condition (no siRNA transfection). Experiments were performed in independent
820 biological triplicates (MALAT1) and quadruplicates (ING2). Data are presented as mean (SD).
821 Unpaired *t*-test with Welch's correction were performed. The statistical significance is
822 **P=0,0019 (NT *vs* siCTL); NS= non-significant (P=0,1755); ***P=0,0001 (NT *vs* siWDR91);
823 ****P<0,0001 (NT *vs* siCTL).

824

825 **Figure 7. Functional validation of WDR91 in an immortalized DMD muscle cell line**
826 **(KM571).** (A) Experimental setup for the double transfection protocol of siRNAs and SSOs in
827 KM571 (B) *WDR91* and *ANXA2* mRNAs silencing efficiency (siCTL: Control siRNA) (C)
828 *WDR91* and *ANXA2* mRNAs silencing effects on exon 51 skipping efficiency of the SSOEx51
829 (D) Experimental setup for the double transfection protocol of siRNAs and a GM against
830 MALAT1 (GM MALAT1) in KM571 (E) *WDR91* and *ANXA2* mRNAs silencing efficiency
831 (siCTL: Control siRNA) (F) *WDR91* and *ANXA2* mRNAs silencing effects on MALAT1
832 knockdown induced by the GM MALAT1. Results are shown as the average of at least four
833 independent biological replicates. Data are presented as mean (SD). The relative mRNA fold
834 change was normalized to the appropriate control condition (Mock or siCTL). Unpaired *t*-test

835 with Welch's correction were performed. The statistical significance is ** P <0,005;
836 ****P<0,00005.

837

838 **Supplemental Figure S1. Gene set enrichment analysis on activator candidates.** Gene set
839 enrichment analysis using PANGEA (Pathway, Network and Gene-set Enrichment Analysis)
840 allowed to classify the activator candidates based on the cellular component gene ontology.
841 Each gene set is classified according to its highest value (log2 fold change). In green are framed
842 the proteins that are part of the peroxisome cellular component. In red are framed the proteins
843 that are part of the mitochondrion cellular component. In purple are framed the proteins that are
844 part of the actin cytoskeleton cellular component. The color code and corresponding lines
845 highlight common candidates between each corresponding cellular component.

846

847 **Supplemental Figure S2. Gene set enrichment analysis on inhibitor candidates.** Gene set
848 enrichment analysis using PANGEA (Pathway, Network and Gene-set Enrichment Analysis)
849 allowed to classify the inhibitor candidates based on the cellular component gene ontology.
850 Each gene set is classified according to its highest value (log2 fold change). In green are framed
851 the proteins that are part of the Golgi apparatus cellular component. In red are framed the
852 proteins that are part of the microtubule cytoskeleton cellular component. In purple are framed
853 the proteins that are part of the endosomal cellular component. The color code and
854 corresponding lines highlight common candidates between each corresponding cellular
855 component.

856

857 **Supplemental Figure S3.** (A) Western blot analysis of ANXA2 protein expression at 48h and
858 72h on non-treated 501Mel cells and after ANXA2 or control siRNA reverse transfections. NT:

859 non-treated; siANXA2: ANXA2 siRNA; siCTL: Negative control siRNA. Alpha-tubulin was
860 used as a loading control (B) Evaluation and quantification of the candidate's knockdown
861 efficiency by RT-qPCR on total RNAs coming from non-treated (NT) or siRNA transfected
862 501Mel cells. Data are calculated from three technical replicates. % knockdown (KD) was
863 calculated as $100*(1-2^{-ddCt})$. TBP was used as housekeeping gene (C) TYRP1 mRNA
864 quantification by RT-qPCR on total RNAs coming from non-treated (NT) or siRNA transfected
865 501Mel cells (CTL: control siRNA). Results are shown as the mean of at least three independent
866 biological replicates (SD).

867

868 **Supplemental Figure S4. WDR91 do not affect the activity of a methoxyethyl chemistry**
869 **splice switching oligonucleotide in DMD muscle cells.** SSOEx51 used in these experiments
870 is an 2MOE PS. (A) *WDR91* and *ANXA2* mRNAs silencing efficiency (siCTL: Control siRNA)
871 (B) *WDR91* and *ANXA2* mRNAs silencing effects on exon 51 skipping efficacy of the SSOEx51
872 2MOE PS. Results are shown as the average of at least four independent biological replicates.
873 Data are presented as mean (SD). The relative mRNA fold change was normalized to the
874 appropriate control condition (Mock or siCTL). P-value was calculated by two-sided unpaired
875 t-tests against the Mock transfected or control siRNA condition. The statistical significance is
876 ** $P < 0.005$; ****$P < 0.00005$.

877

878

879

880

881

882 **Table 1. List of the ASO activator and inhibitor candidates sorted after applying M, A**

883 **and fold change filters.**

sgRNA activator candidates - 4 guides (A ≥ 6 and M ≥ 0.6)							
guide	**M**	**A**	**d**	**KO**	**CTL**	**TRT**	**FC**
sgELMOD1-1	0,6958466	7,2667865	75	322	121	196	1,6198347
sgELMOD1-2	0,6369571	8,0866629	121	361	218	339	1,5550459
sgELMOD1-3	0,6235261	8,4564213	153	393	283	436	1,540636
sgELMOD1-4	1,5292531	7,2240582	166	178	88	254	2,8863636
sgFH-1	0,6053303	9,0237643	220	718	422	642	1,521327
sgFH-2	0,7281282	8,3974871	172	327	262	434	1,6564885
sgFH-3	1,2947433	7,8761903	218	369	150	368	2,4533333
sgFH-4	0,8187178	8,4915079	207	249	271	478	1,7638376
sgSMOX-1	0,7555813	7,6445772	106	171	154	260	1,6883117
sgSMOX-2	0,6197279	8,667416	176	474	328	504	1,5365854
sgSMOX-3	0,7618403	8,2264102	160	190	230	390	1,6956522
sgSMOX-4	0,9798221	7,9817642	175	318	180	355	1,9722222
sgTADA2B-1	0,8148755	8,7649898	249	281	328	577	1,7591463
sgTADA2B-2	0,8802608	9,8452718	570	821	678	1248	1,840708
sgTADA2B-3	1,2351554	8,3249368	283	295	209	492	2,354067
sgTADA2B-4	0,9574395	7,9049845	162	213	172	334	1,9418605
sgWBSCR16-	1,4890381	6,5774091	103	171	57	160	2,8070175
sgWBSCR16-	0,9309584	7,2069462	97	228	107	204	1,9065421
sgWBSCR16-	1,4317162	6,1421229	73	408	43	116	2,6976744
sgWBSCR16-	1,2064509	7,8886277	204	451	156	360	2,3076923
sgRNA activator candidates - 3 guides (A ≥ 6 and M ≥ 0.6)							
guide	**M**	**A**	**d**	**KO**	**CTL**	**TRT**	**FC**
sgACOX1-1	1,0865877	7,1432067	109	91	97	206	2,1237113
sgACOX1-2	0,8549069	8,7673034	262	655	324	586	1,808642
sgACOX1-4	1,1933439	8,6078992	332	416	258	590	2,2868217
sgAUH-2	0,7324145	8,3548919	168	472	254	422	1,6614173
sgAUH-3	0,6228424	9,0461308	230	528	426	656	1,5399061
sgAUH-4	0,6529393	9,1593597	261	619	456	717	1,5723684
sgZNF189-2	0,6429894	8,7008731	187	398	333	520	1,5615616
sgZNF189-3	0,6571123	7,350924	75	195	130	205	1,5769231
sgZNF189-4	0,6205347	9,1368159	244	618	454	698	1,5374449
sgC7-1	0,5912488	8,1348282	116	513	229	345	1,5065502
sgC7-2	0,6367837	8,6358045	177	274	319	496	1,5548589
sgC7-4	0,8353035	8,3305411	189	333	241	430	1,7842324
sgCEP250-1	0,6247301	9,2460557	265	430	489	754	1,5419223
sgCEP250-2	0,7260548	9,552852	382	664	584	966	1,6541096
sgCEP250-4	0,8147345	8,0146975	148	367	195	343	1,7589744
sgCOG8-1	0,8910656	7,2268925	94	367	110	204	1,8545455
sgCOG8-3	0,8728881	6,8114835	69	249	83	152	1,8313253
sgCOG8-4	0,9569313	6,8878566	80	174	85	165	1,9411765

sgCREB1-1	0,7116545	7,4643517	88	248	138	226	1,6376812
sgCREB1-3	0,9640804	7,4127776	116	309	122	238	1,9508197
sgCREB1-4	0,6993405	7,0078817	63	159	101	164	1,6237624
sgZFHX2-2	0,7837915	7,9918086	140	337	194	334	1,7216495
sgZFHX2-3	1,3598959	6,5868386	94	130	60	154	2,5666667
sgZFHX2-4	0,9162611	7,513413	118	236	133	251	1,887218
sgFAM168B-1	0,9298122	7,9487219	162	278	179	341	1,9050279
sgFAM168B-2	0,8813555	7,8585303	144	222	171	315	1,8421053
sgFAM168B-3	0,9203406	8,3790335	216	356	242	458	1,892562
sgFAM25C-1	0,6313554	6,988103	56	254	102	158	1,5490196
sgFAM25C-3	0,9268336	6,9712114	82	317	91	173	1,9010989
sgFAM25C-4	0,6568964	7,6771764	94	162	163	257	1,5766871
sgGRIK1-1	1,1431538	7,690518	168	247	139	307	2,2086331
sgGRIK1-2	0,7316124	7,7056562	107	276	162	269	1,6604938
sgGRIK1-3	1,4253058	6,8419359	118	218	70	188	2,6857143
sgHAND1-1	0,7300379	7,7487232	110	181	167	277	1,6586826
sgHAND1-2	0,9682911	7,0077075	88	112	92	180	1,9565217
sgHAND1-4	1,3823007	7,5615151	188	330	117	305	2,6068376
sgHEATR5B-	0,9083113	8,1194916	178	317	203	381	1,8768473
sgHEATR5B-	0,7393781	8,2705559	160	367	239	399	1,6694561
sgHEATR5B-	1,1006324	8,5892352	301	616	263	564	2,1444867
sgHOXC9-1	0,6398244	7,3311395	72	216	129	201	1,5581395
sgHOXC9-2	0,7583174	8,9827851	269	585	389	658	1,6915167
sgHOXC9-4	0,650254	7,495052	82	318	144	226	1,5694444
sgHSD17B4-1	0,6453351	8,7779948	198	452	351	549	1,5641026
sgHSD17B4-2	0,7154095	9,2403478	303	795	472	775	1,6419492
sgHSD17B4-3	1,2322909	6,9911849	112	80	83	195	2,3493976
sgXYLT2-1	1,325958	8,8228503	431	421	286	717	2,506993
sgXYLT2-2	0,6378574	9,2318181	268	547	482	750	1,5560166
sgXYLT2-3	0,6796212	8,7868938	210	264	349	559	1,6017192
sgLMOD2-1	0,6520767	8,3033183	144	542	252	396	1,5714286
sgLMOD2-3	0,6694844	8,731347	199	572	337	536	1,5905045
sgLMOD2-4	1,0959244	8,4548528	273	480	240	513	2,1375
sgMAP2-2	0,617328	7,8860928	102	477	191	293	1,5340314
sgMAP2-3	0,5981194	9,1847561	243	482	473	716	1,5137421
sgMAP2-4	1,0140752	8,501391	260	472	255	515	2,0196078
sgPAK2-1	0,7918918	8,7839632	245	459	335	580	1,7313433
sgPAK2-3	0,980778	8,8997799	331	435	340	671	1,9735294
sgPAK2-4	1,1615891	7,6576102	167	334	135	302	2,237037
sgPCNP-2	1,549687	6,883368	133	232	69	202	2,9275362
sgPCNP-3	1,8875253	6,2656907	108	42	40	148	3,7
sgPCNP-4	0,6305033	8,7373164	188	441	343	531	1,548105
sgSAYSD1-1	0,8573116	8,2295557	181	279	223	404	1,8116592
sgSAYSD1-2	1,2669389	7,5759839	173	204	123	296	2,4065041
sgSAYSD1-3	0,8245233	7,8960774	138	381	179	317	1,7709497
sgTAF4B-2	1,0236513	7,4306889	125	180	121	246	2,0330579

sgTAF4B-3	0,9853532	8,1220332	194	331	198	392	1,979798
sgTAF4B-4	0,8975844	8,070844	170	408	197	367	1,8629442
sgTAMM41-1	0,6133909	7,3727846	71	310	134	205	1,5298507
sgTAMM41-3	0,8081693	8,3870782	190	313	253	443	1,7509881
sgTAMM41-4	0,8866182	7,8695739	146	627	172	318	1,8488372
sgTEK-2	1,0785691	7,6053737	149	195	134	283	2,1119403
sgTEK-3	0,6268466	9,0616161	234	573	430	664	1,544186
sgTEK-4	0,9549761	7,9613038	168	301	179	347	1,9385475
sgTMPRSS13-	1,1076683	8,9716867	395	531	342	737	2,1549708
sgTMPRSS13-	0,6516536	8,6019512	177	520	310	487	1,5709677
sgTMPRSS13-	0,6668322	9,1503997	265	827	451	716	1,5875831
sgTOR1AIP1-	0,8596273	8,6682184	246	488	302	548	1,8145695
sgTOR1AIP1-	0,8280875	8,2405923	176	215	227	403	1,7753304
sgTOR1AIP1-	2,1609919	6,2504209	125	99	36	161	4,4722222
sgUTS2B-2	0,9805825	8,0371857	182	376	187	369	1,973262
sgUTS2B-3	0,6425732	8,8131397	202	283	360	562	1,5611111
sgUTS2B-4	0,7680761	8,9036743	258	552	367	625	1,7029973
sgVMP1-1	1,4499357	7,3248807	168	439	97	265	2,7319588
sgVMP1-2	0,8605969	5,678226	31	256	38	69	1,8157895
sgVMP1-4	1,3168571	6,4913186	85	286	57	142	2,4912281
sgRNA activator candidates 2 guides (A ≥ 6 and M ≥ 0.6)							
guide	**M**	**A**	**d**	**KO**	**CTL**	**TRT**	**FC**
sgACOX1-1	1,0865877	7,1432067	109	91	97	206	2,1237113
sgACOX1-4	1,1933439	8,6078992	332	416	258	590	2,2868217
sgACVR1B-3	1,007342	8,1183808	198	357	196	394	2,0102041
sgACVR1B-4	1,2302976	6,3155885	70	105	52	122	2,3461538
sgAXIN1-1	1,6241686	7,7309475	252	162	121	373	3,0826446
sgAXIN1-4	1,0143553	7,7359963	153	225	150	303	2,02
sgBRI3BP-1	1,0336593	8,3810158	244	273	233	477	2,0472103
sgBRI3BP-2	1	6,6085245	69	72	69	138	2
sgBSND-2	1,2103599	8,0314447	226	387	172	398	2,3139535
sgBSND-4	1,9125372	6,0437314	94	132	34	128	3,7647059
sgCBWD6-2	1,1885777	7,3887047	142	295	111	253	2,2792793
sgCBWD6-3	1,0703893	7,1790509	110	580	100	210	2,1
sgCCDC65-1	1,277781	6,8287151	104	258	73	177	2,4246575
sgCCDC65-4	1,7045441	6,6071596	122	212	54	176	3,2592593
sgCCL4L2-2	1,0404791	7,462754	130	359	123	253	2,0569106
sgCCL4L2-4	1,4150375	7,7843343	225	269	135	360	2,6666667
sgCDC42-2	1,7288377	7,3401523	206	417	89	295	3,3146067
sgCDC42-4	1,1139562	6,7468027	85	505	73	158	2,1643836
sgCHERP-3	1,0324215	7,2975705	115	535	110	225	2,0454545
sgCHERP-4	1,1667784	7,2558146	127	368	102	229	2,245098
sgCHURC1-	1,1016954	7,0265811	102	718	89	191	2,1460674
sgCHURC1-	1,4739312	6,7142455	112	611	63	175	2,7777778
sgCIAO1-3	1,0588937	6,9217643	91	519	84	175	2,0833333
sgCIAO1-4	1,5215371	6,7149649	116	452	62	178	2,8709677

sgCNR1-2	1,017848	8,4218133	247	375	241	488	2,0248963
sgCNR1-3	1,122374	8,8138524	359	320	305	664	2,1770492
sgCSTB-3	1,16711	7,416445	142	354	114	256	2,245614
sgCSTB-4	1,5077946	6,7538973	118	252	64	182	2,84375
sgDEFB135-1	1,4139572	8,0906829	278	358	167	445	2,6646707
sgDEFB135-4	1,0584597	7,5845123	144	330	133	277	2,0827068
sgEED-1	1,1737366	7,9791857	211	466	168	379	2,2559524
sgEED-2	1,4666199	8,2411046	321	217	182	503	2,7637363
sgERVFRD-1-	1,1425391	7,5936374	157	138	130	287	2,2076923
sgERVFRD-1-	1,0366585	7,6057921	143	227	136	279	2,0514706
sgEXT2-1	1,0484101	9,9208098	720	908	674	1394	2,0682493
sgEXT2-2	1,1969155	8,5814513	327	352	253	580	2,2924901
sgEXTL3-2	1,3345683	9,6330684	761	352	500	1261	2,522
sgEXTL3-3	1,2886643	9,9274205	899	515	623	1522	2,4430177
sgFANCC-2	1,2113089	7,9979719	221	191	168	389	2,3154762
sgFANCC-3	1,3475043	7,6162667	190	205	123	313	2,5447154
sgFIS1-1	1,052321	7,9855921	189	424	176	365	2,0738636
sgFIS1-3	1,8405218	6,3465256	111	731	43	154	3,5813953
sgGABBR1-1	1,1755716	7,9971767	214	213	170	384	2,2588235
sgGABBR1-4	1,0378682	8,0735229	198	305	188	386	2,0531915
sgGRIK1-1	1,1431538	7,690518	168	247	139	307	2,2086331
sgGRIK1-3	1,4253058	6,8419359	118	218	70	188	2,6857143
sgHNRNPF-1	1,3219281	6,3048202	75	205	50	125	2,5
sgHNRNPF-4	1,5484366	6,0961464	77	139	40	117	2,925
sgHNRNPL-3	2,0202724	6,7380567	162	362	53	215	4,0566038
sgHNRNPL-4	1,3572951	8,7766797	428	848	274	702	2,5620438
sgICOSLG-3	1,0783162	8,4580214	269	333	242	511	2,1115702
sgICOSLG-4	1,1982696	7,4064897	145	272	112	257	2,2946429
sgKRTAP4-9-	1,7432246	6,3951742	108	229	46	154	3,3478261
sgKRTAP4-9-	1,177193	7,0480281	111	179	88	199	2,2613636
sgLCP1-1	1,0192791	8,3105394	229	303	223	452	2,0269058
sgLCP1-2	1,2638123	8,9033692	433	468	309	742	2,4012945
sgMCM5-1	1,4277486	7,5340532	191	527	113	304	2,6902655
sgMCM5-2	1,3393853	7,5151827	176	522	115	291	2,5304348
sgMETAP1-1	1,0553768	7,3731784	124	349	115	239	2,0782609
sgMETAP1-4	1,1938797	6,7867644	94	364	73	167	2,2876712
sgNKX2-4-2	1,0571954	7,6160605	147	173	136	283	2,0808824
sgNKX2-4-3	1,020716	8,4292212	249	260	242	491	2,0289256
sgNRD1-1	1,2446739	8,6279615	352	480	257	609	2,3696498
sgNRD1-4	1,2132032	7,6834172	178	325	135	313	2,3185185
sgOLFML3-1	1,284096	7,0514389	122	329	85	207	2,4352941
sgOLFML3-4	1,5398105	7,664723	227	262	119	346	2,907563
sgOR2L5-3	1,4742034	8,4650221	377	422	212	589	2,7783019
sgOR2L5-4	1,1604647	6,6676952	84	56	68	152	2,2352941
sgOR4C12-3	1,2410081	6,8872906	105	214	77	182	2,3636364
sgOR4C12-4	1,0074175	8,6885841	294	388	291	585	2,0103093

sgPKLR-1	1,254138	7,5578063	169	220	122	291	2,3852459
sgPKLR-4	1,0901978	7,0842577	105	322	93	198	2,1290323
sgPOC1A-1	1,3219281	6,8704174	111	240	74	185	2,5
sgPOC1A-4	1,0402639	7,2480524	112	495	106	218	2,0566038
sgPOF1B-2	1,226915	7,1212521	122	146	91	213	2,3406593
sgPOF1B-4	1,4065059	7,4311734	175	269	106	281	2,6509434
sgPRSS53-2	1,1643868	7,0251369	108	183	87	195	2,2413793
sgPRSS53-3	1,4489848	6,7017723	109	131	63	172	2,7301587
sgPSMA1-2	1,0631938	6,5976861	73	345	67	140	2,0895522
sgPSMA1-4	1,2644156	7,0751513	122	273	87	209	2,4022989
sgPTP4A1-1	1,6114347	6,5606049	111	181	54	165	3,0555556
sgPTP4A1-2	1,2337972	6,3717861	73	108	54	127	2,3518519
sgRERE-1	1,6412699	6,8867242	142	366	67	209	3,119403
sgRERE-4	1,3136605	7,3710758	156	195	105	261	2,4857143
sgRPS14-2	3,5443205	3,3571228	32	28	3	35	11,666667
sgRPS14-3	1,5589673	6,5868386	109	243	56	165	2,9464286
sgSLC35B1-1	1,3362834	8,5750323	366	911	240	606	2,525
sgSLC35B1-4	1,4329594	6,0384078	68	217	40	108	2,7
sgSLC39A9-3	1,0524674	7,6030493	145	438	135	280	2,0740741
sgSLC39A9-4	1,0193468	10,527874	1065	901	1037	2102	2,027001
sgSLC5A7-1	1,0329146	6,5388251	68	112	65	133	2,0461538
sgSLC5A7-3	1,1043367	8,4590589	276	382	240	516	2,15
sgSOD2-1	1,4296843	7,329552	166	160	98	264	2,6938776
sgSOD2-3	1,3219281	6,3048202	75	191	50	125	2,5
sgSPDYE2-1	1,017403	8,1952021	211	341	206	417	2,0242718
sgSPDYE2-3	1,0740006	6,7849278	84	477	76	160	2,1052632
sgSRF-2	2,194378	5,7976287	93	594	26	119	4,5769231
sgSRF-4	1,4788341	6,2940059	84	293	47	131	2,787234
sgSTK32B-1	1,3245252	7,4566785	167	270	111	278	2,5045045
sgSTK32B-2	1,4484605	7,3091928	166	294	96	262	2,7291667
sgTELO2-1	1,0919225	6,7938888	86	424	76	162	2,1315789
sgTELO2-2	1,1443899	6,405085	69	576	57	126	2,2105263
sgTLCD1-2	1,2459792	6,9083918	107	169	78	185	2,3717949
sgTLCD1-3	1,0673553	7,6211405	149	378	136	285	2,0955882
sgTMC7-2	1,9237644	6,049345	95	56	34	129	3,7941176
sgTMC7-4	1,1375035	7,1386074	114	397	95	209	2,2
sgTMEM131-	1,3487282	6,6743641	99	243	64	163	2,546875
sgTMEM131-	1,1672947	6,5143847	76	189	61	137	2,2459016
sgUBALD1-2	1,0038116	8,0641482	190	269	189	379	2,005291
sgUBALD1-4	1,0949484	7,7471465	167	569	147	314	2,1360544
sgUQCRB-3	1,5849625	6,573841	110	240	55	165	3
sgUQCRB-4	1,0448542	8,0922827	202	386	190	392	2,0631579
sgVMP1-1	1,4499357	7,3248807	168	439	97	265	2,7319588
sgVMP1-4	1,3168571	6,4913186	85	286	57	142	2,4912281
sgVSTM5-3	1,3138908	6,8268704	107	236	72	179	2,4861111
sgVSTM5-4	1,3858912	6,9217643	121	240	75	196	2,6133333

sgWDR91-1	1,7766218	6,8190482	148	69	61	209	3,4262295
sgWDR91-3	1,6002524	8,5749132	445	277	219	664	3,0319635
sgZNF492-2	1,2505435	7,4832527	160	217	116	276	2,3793103
sgZNF492-3	1,1901029	6,7447986	91	275	71	162	2,2816901
sgZNRD1-1	1,8559897	6,571851	131	635	50	181	3,62
sgZNRD1-4	1,3706434	7,3146783	157	412	99	256	2,5858586
sgRNA inhibitor candidates - 4 guides (A ≥ 6 and M ≤ -0.6)							
guide	**M**	**A**	**d**	**KO**	**CTL**		**FC**
sgGGTLC2-1	-1,230298	7,3155885	-140	301	244	104	2,3461538
sgGGTLC2-2	-1,380822	7,8603359	-231	287	375	144	2,6041667
sgGGTLC2-3	-0,924232	8,2103091	-193	230	408	215	1,8976744
sgGGTLC2-4	-0,748292	8,0394819	-138	374	341	203	1,679803
sgMTUS2-1	-1,366782	4,9313187	-30	100	49	19	2,5789474
sgMTUS2-2	-1,090198	6,4992952	-70	157	132	62	2,1290323
sgMTUS2-3	-1,411314	7,30557	-161	348	258	97	2,6597938
sgMTUS2-4	-0,59172	6,4456071	-36	156	107	71	1,5070423
sgNKAIN4-1	-0,787885	8,9369743	-271	616	644	373	1,7265416
sgNKAIN4-2	-1,308922	8,9398634	-461	460	773	312	2,4775641
sgNKAIN4-3	-1,04891	7,9673983	-186	220	360	174	2,0689655
sgNKAIN4-4	-1,554589	5,7772944	-62	55	94	32	2,9375
sgRNA inhibitor candidates - 3 guides (A ≥ 6 and M ≤ -0.6)							
guide	**M**	**A**	**d**	**KO**	**CTL**		**FC**
sgAATF-1	-1,301464	6,8004791	-104	239	175	71	2,4647887
sgAATF-2	-0,619095	7,8093935	-97	195	278	181	1,5359116
sgAATF-3	-1,47592	7,1809034	-155	419	242	87	2,7816092
sgBOLA2-1	-1,657112	7,9884275	-308	121	451	143	3,1538462
sgBOLA2-2	-1,194816	6,9724475	-107	255	190	83	2,2891566
sgBOLA2-3	-0,610498	7,1126037	-59	322	171	112	1,5267857
sgCABP2-1	-1,247928	7,6239638	-176	350	304	128	2,375
sgCABP2-3	-1,152599	7,4951628	-148	386	269	121	2,2231405
sgCABP2-4	-0,753839	7,049345	-70	249	172	102	1,6862745
sgCCDC102A-	-1,078003	7,9568538	-190	378	361	171	2,1111111
sgCCDC102A-	-0,740913	6,5602809	-49	61	122	73	1,6712329
sgCCDC102A-	-1,436099	6,8055124	-116	218	184	68	2,7058824
sgKARS-1	-1,417767	8,3382403	-331	548	529	198	2,6717172
sgKARS-2	-1,609416	6,09011	-80	566	119	39	3,0512821
sgKARS-3	-1,494765	5,7917765	-60	447	93	33	2,8181818
sgSLITRK3-1	-1,426265	7,2980949	-162	172	258	96	2,6875
sgSLITRK3-2	-1,176453	9,2029364	-494	873	886	392	2,2602041
sgSLITRK3-3	-0,63743	9,48864	-320	744	896	576	1,5555556
sgL1CAM-1	-1,093867	7,4417512	-135	161	254	119	2,1344538
sgL1CAM-2	-1,788872	7,5526474	-248	238	349	101	3,4554455
sgL1CAM-3	-0,606336	8,9542198	-210	422	612	402	1,5223881
sgRNA inhibitor candidates - 2 guides (A ≥ 6 and M ≤ -0.6)							
guide	**M**	**A**	**d**	**KO**	**CTL**		**FC**
sgACOT8-2	-1,182864	6,8008854	-94	124	168	74	2,2702703

sgACOT8-3	-1,214878	7,9737614	-218	274	383	165	2,3212121
sgARHGEF2-	-1,186096	7,7015726	-176	275	314	138	2,2753623
sgARHGEF2-	-1,246966	7,9272638	-217	357	375	158	2,3734177
sgCASP5-3	-1,04182	7,1933354	-108	208	210	102	2,0588235
sgCASP5-4	-1,285909	6,832779	-105	160	178	73	2,4383562
sgCCDC51-2	-1,284453	7,5125914	-168	185	285	117	2,4358974
sgCCDC51-4	-1,059334	7,5630901	-142	97	273	131	2,0839695
sgCLEC18C-1	-1,657112	4,5289959	-28	63	41	13	3,1538462
sgCLEC18C-3	-1,232661	7,2601866	-135	239	235	100	2,35
sgFAM86B1-2	-1,153079	6,6426289	-82	238	149	67	2,2238806
sgFAM86B1-4	-1,395929	7,2678199	-155	312	250	95	2,6315789
sgKRT20-2	-0,763197	8,1497829	-152	368	370	218	1,6972477
sgKRT20-3	-0,604862	6,8873935	-50	403	146	96	1,5208333
sgLILRA6-1	-1,079727	6,9992952	-98	142	186	88	2,1136364
sgLILRA6-4	-1,04858	8,2990771	-234	447	453	219	2,0684932
sgMRPL52-1	-1,398549	7,4806344	-180	379	290	110	2,6363636
sgMRPL52-4	-1,021695	6,5552417	-68	249	134	66	2,030303
sgNEDD8-3	-2,807355	3,7256056	-30	633	35	5	7
sgNEDD8-4	-1,258734	7,4367221	-156	570	268	112	2,3928571
sgNELFB-2	-0,671578	7,7194934	-99	396	266	167	1,5928144
sgNELFB-4	-2,004738	7,2502965	-229	480	305	76	4,0131579
sgRDH11-1	-1,291582	8,4336937	-320	341	541	221	2,4479638
sgRDH11-2	-1,224291	8,3736966	-290	191	507	217	2,3364055
sgSF3A2-2	-1,065724	7,4155051	-129	116	247	118	2,0932203
sgSF3A2-4	-1,050626	7,332668	-120	411	232	112	2,0714286
sgSNAPC4-1	-1,104337	4,8740964	-23	225	43	20	2,15
sgSNAPC4-2	-1,563429	7,2735678	-176	304	266	90	2,9555556
sgSSRP1-1	-1,20581	6,8317235	-98	226	173	75	2,3066667
sgSSRP1-2	-1,179133	8,7941377	-373	425	668	295	2,2644068
sgTUBG1-3	-1,252387	5,7136564	-47	304	81	34	2,3823529
sgTUBG1-4	-1,163348	7,9995265	-212	729	383	171	2,2397661
sgGOLGA8N-	-1,39486	7,4523173	-176	165	284	108	2,6296296
sgGOLGA8N-	-1,389042	6,6718011	-102	199	165	63	2,6190476
sgHMBS-1	-1,00946	6,7526577	-77	222	153	76	2,0131579
sgHMBS-4	-1,39486	7,0372798	-132	218	213	81	2,6296296
sgKLK14-1	-0,85561	7,6274774	-119	276	266	147	1,8095238
sgKLK14-4	-1,092824	7,8501928	-179	347	337	158	2,1329114
sgMFAP1-1	-1,348895	6,402368	-82	246	135	53	2,5471698
sgMFAP1-3	-1,463947	6,5899545	-102	222	160	58	2,7586207
sgNDUFAB1-	-1,096215	5,4060887	-33	87	62	29	2,137931
sgNDUFAB1-	-1,777608	6,6961587	-136	257	192	56	3,4285714
sgNKIRAS2-3	-1,836501	6,7256056	-144	170	200	56	3,5714286
sgNKIRAS2-4	-1,24664	6,505963	-81	175	140	59	2,3728814
sgNPR3-1	-1,353637	7,6540984	-196	301	322	126	2,5555556
sgNPR3-2	-1,123896	8,0855102	-217	378	401	184	2,1793478
sgPAIP2-3	-1,592825	6,7271496	-123	27	184	61	3,0163934

sgPAIP2-4	-2,365181	6,7061526	-191	99	237	46	5,1521739
sgREEP2-2	-1,192645	8,0475337	-225	139	400	175	2,2857143
sgREEP2-4	-1,007777	8,0352701	-187	259	372	185	2,0108108
sgRSPH6A-1	-1,597563	6,0467088	-77	120	115	38	3,0263158
sgRSPH6A-4	-1,524421	7,952035	-274	270	420	146	2,8767123
sgTCEA3-1	-1,5025	6,1435676	-77	184	119	42	2,8333333
sgTCEA3-2	-1,185279	7,6694552	-172	166	307	135	2,2740741
sgTMEM14C-	-1,073249	8,121587	-212	382	404	192	2,1041667
sgTMEM14C-	-1,523562	7,2212126	-165	287	253	88	2,875
sgTRAFD1-1	-1,463247	7,4181238	-181	309	284	103	2,7572816
sgTRAFD1-4	-1,119299	6,4176305	-68	108	126	58	2,1724138
sgUGCG-1	-1,065095	6,5549153	-71	179	136	65	2,0923077
sgUGCG-2	-1,649379	7,0145142	-156	77	229	73	3,1369863
sgWDR12-1	-2,039528	6,9970441	-196	248	259	63	4,1111111
sgWDR12-3	-1,534777	6,0527906	-74	93	113	39	2,8974359
sgN6AMT2-1	-1,532495	7,8955306	-265	138	405	140	2,8928571
sgN6AMT2-3	-1,214682	7,67343	-177	152	311	134	2,3208955
sgNLRC3-2	-1,504994	6,8399599	-125	88	193	68	2,8382353
sgNLRC3-3	-1,117039	6,7082668	-83	216	154	71	2,1690141
sgPLA2G7-1	-3,006919	6,2038994	-183	191	209	26	8,0384615
sgPLA2G7-2	-1,389706	7,9986339	-256	318	414	158	2,6202532
sgPSENEN-3	-1,20112	8,5312971	-317	490	561	244	2,2991803
sgPSENEN-4	-1,420181	7,4243359	-176	470	281	105	2,6761905
sgRSF1-1	-1,030261	9,162589	-418	640	819	401	2,042394
sgRSF1-4	-1,193604	7,1513909	-121	178	215	94	2,287234
sgSTK11-1	-1,217029	6,8753012	-102	386	179	77	2,3246753
sgSTK11-4	-1,237039	6,7478026	-95	236	165	70	2,3571429
sgTMPRSS2-2	-1,188762	7,1335396	-119	159	212	93	2,2795699
sgTMPRSS2-3	-1,273018	6,5433998	-85	96	145	60	2,4166667
sgXKR4-2	-1,347019	6,5063996	-88	185	145	57	2,5438596
sgXKR4-3	-1,072569	7,5135642	-139	341	265	126	2,1031746
sgBBIP1-2	-1,407175	6,2271496	-76	130	122	46	2,6521739
sgBBIP1-4	-1,591915	6,9044821	-139	211	208	69	3,0144928
sgATP6V0D2-	-1,051193	8,5645157	-282	303	545	263	2,0722433
sgATP6V0D2-	-1,341037	6,8993371	-115	75	190	75	2,5333333
sgBCL10-3	-1,532221	6,7884783	-123	218	188	65	2,8923077
sgBCL10-4	-1,028855	7,1437841	-103	137	202	99	2,040404
sgC1orf158-1	-1,181838	8,9789364	-425	422	760	335	2,2686567
sgC1orf158-4	-1,007777	8,0352701	-187	289	372	185	2,0108108
sgCPSF4L-2	-0,554031	8,058375	-103	314	323	220	1,4681818
sgCPSF4L-4	-1,241376	7,8590925	-206	318	357	151	2,3642384
sgFLVCR2-3	-1,053111	8,6558387	-301	515	581	280	2,075
sgFLVCR2-4	-1,525827	7,1379531	-156	218	239	83	2,8795181

The corresponding 95 and 55 activator and inhibitor candidates are represented with their respective sgRNAs fulfilling the defined criteria. M (log ratio) = log2(sgRNA_count_in_TRT+1) -

886 log2(sgRNA_count_in_CTL+1); A (Mean average) = mean (count_TRT, count_CTL) in log2 scale. Fold-
887 changes (FC) between TRT (tcT3-treated cells) and CTL (tcC1-treated cells) conditions were computed from
888 the M values of each sgRNA as FC (activator) = TRT read counts / CTL read counts; FC (inhibitor) = CTL
889 read counts / TRT read counts. KO is the number of read counts in the parental non-treated knockout library.
890 d value represents the absolute difference between the CTL and the TRT read counts.

891

892

893

894

895

896

897

898

899

900

901

902

903

904

905

906

907 **Table 2. Raw absorbance at 590nm (crystal violet coloration) of the cell density after four**

908 **days of siRNA or siRNA + tcT3 ASO transfection.**

	NT	NT+tcT3	siCTL	siCTL+tcT3	siWDR91	siWDR91+tcT3
N1	2,251	0,781	1,534	0,403	2,644	1,585
N2	2,93	1,53	2,62	1,19	3,01	2,39
N3	2,89	1,42	ND	ND	2,98	2,42
N4	2,6256	1,0660	1,8022	0,5007	ND	ND
N5	2,8453	1,3494	2,518	1,19	2,927	2,022
N6	2,7067	1,6489	2,229	0,9583	ND	ND
N7	2,2459	ND	1,7195	0,8387	ND	ND
N8	2,2341	ND	2,1565	0,8573	ND	ND

909

	siWBSCR16	siWBSCR16+tcT3	siFH	siFH+tcT3	siELMOD1	siELMOD1+tcT3
N1	2,829	1,4001	2,663	0,767	2,397	0,626
N2	2,79	1,12	ND	ND	ND	ND
N3	3	1,83	ND	ND	ND	ND
N4	ND	ND	ND	ND	ND	ND
N5	ND	ND	ND	ND	ND	ND
N6	ND	ND	ND	ND	ND	ND
N7	2,3493	1,2057	2,8127	1,3581	2,3740	0,4554
N8	2,4994	1,162	2,3923	0,3284	1,8733	0,1822

910

	siTADA2B	siTADA2B+tcT3	siANXA2	siANXA2+tcT3
N1	ND	ND	2,95	2,77
N2	ND	ND	2,69	1,91
N3	ND	ND	ND	ND
N4	1,3038	0,6641	ND	ND
N5	ND	ND	ND	ND
N6	ND	ND	2,3097	2,1038
N7	1,4761	0,8328	2,3289	1,9428
N8	1,663	0,7457	2,3167	1,8059

911 N1 to N8: biological replicates; NT: Non-Treated; siCTL: Control siRNA; ND: Not Determined.

912 **Table 3. Raw absorbance at 590nm (crystal violet coloration) of the cell density after four**

913 **days of siRNA or siRNA + LNA T3 ASO transfection.**

	NT	NT+lnaT3	siCTL	siCTL+lnaT3	siANXA2	siANXA2+lnaT3	siWDR91	siWDR91+lnaT3
N1	2,91	1,9	1,78	0,82	2,42	1,75	2,69	1,65
N2	2,95	2,04	1,91	AM	2,99	2,98	2,92	2,9
N3	2,9	2,43	2,28	1,19	2,85	2,82	2,83	2,82
N4	2,97	2,25	1,15	0,63	2,95	2,87	2,87	1,92
N5	2,9	2,03	1,93	0,94	2,84	2,7	2,77	2,07

914 N1 to N5: biological replicates; NT: Non-Treated; siCTL: Control siRNA; AM: Aberrant Measure.

Figure 1

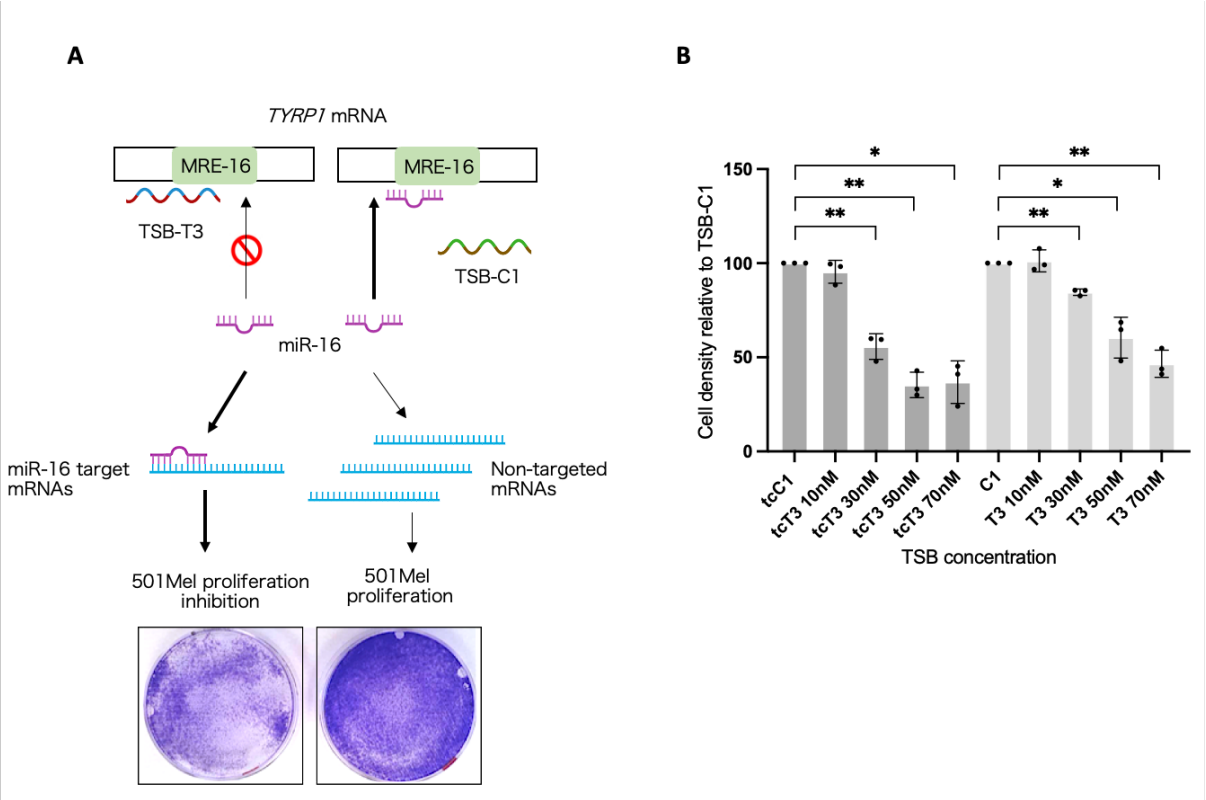
A
TYRP1 mRNA
MRE-16
MRE-16
TSB-T3
TSB-C1
miR-16
miR-16 target mRNAs
Non-targeted mRNAs
501Mel proliferation inhibition
501Mel proliferation
B
Cell density relative to TSB-C1
150
100
50
0
*
**
**
**
*
**
tcC1
tcT3 10nM
tcT3 30nM
tcT3 50nM
tcT3 70nM
C1
T3 10nM
T3 30nM
T3 50nM
T3 70nM
TSB concentration

Figure 2

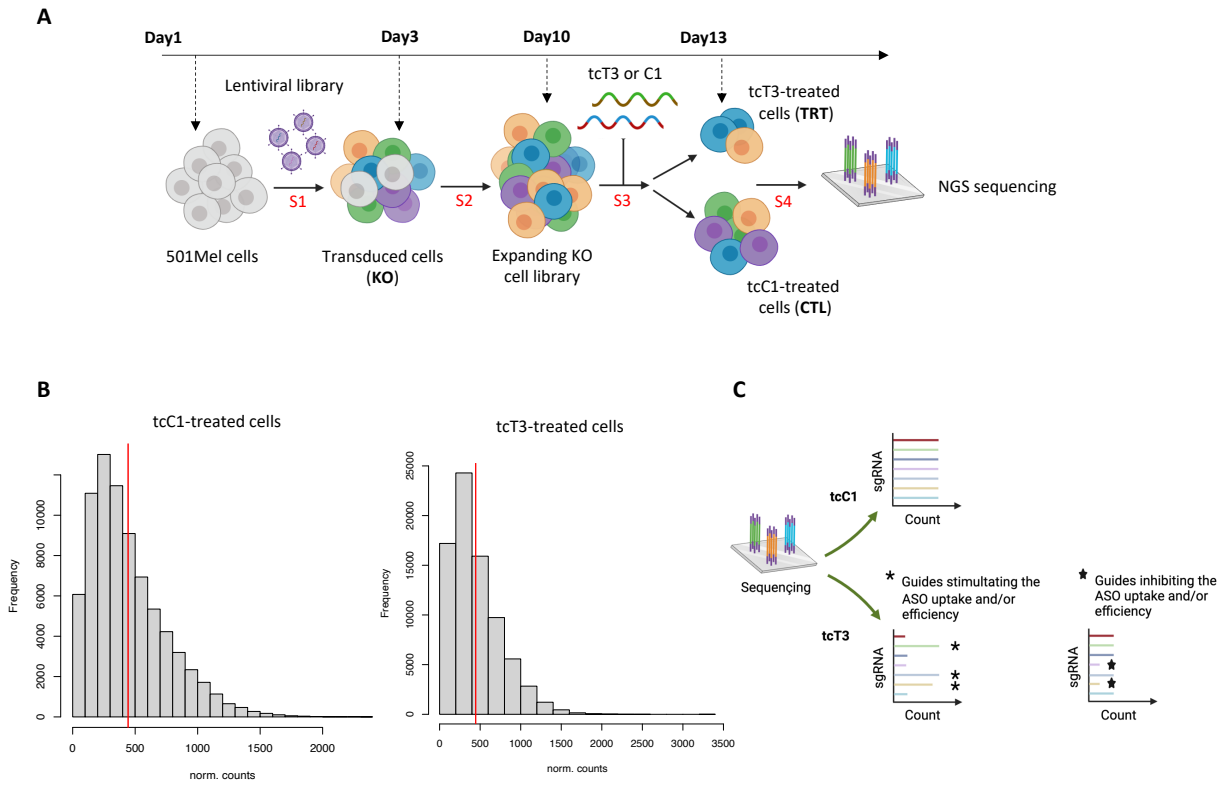
A
Day1
Day3
Day10
Day13
Lentiviral library
tcT3 or C1
tcT3-treated cells (TRT)
S1
S2
S3
S4
NGS sequencing
501Mel cells
Transduced cells (KO)
Expanding KO cell library
tcC1-treated cells (CTL)
B
tcC1-treated cells
tcT3-treated cells
Frequency
norm. counts
C
Sequençing
tcC1
tcT3
sgRNA
Count
Guides stimultating the ASO uptake and/or efficiency
Guides inhibiting the ASO uptake and/or efficiency

Figure 3

A

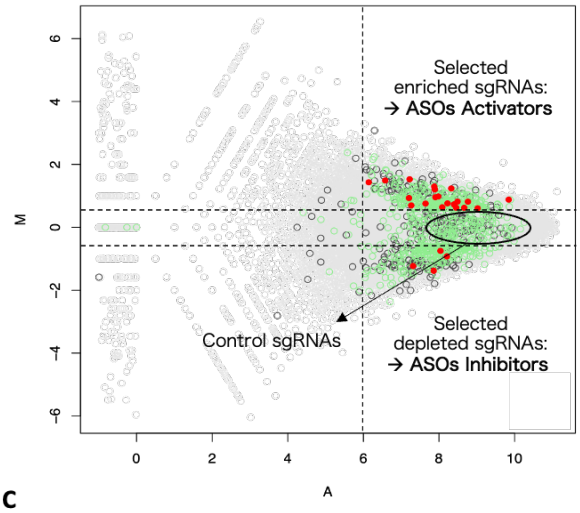

B

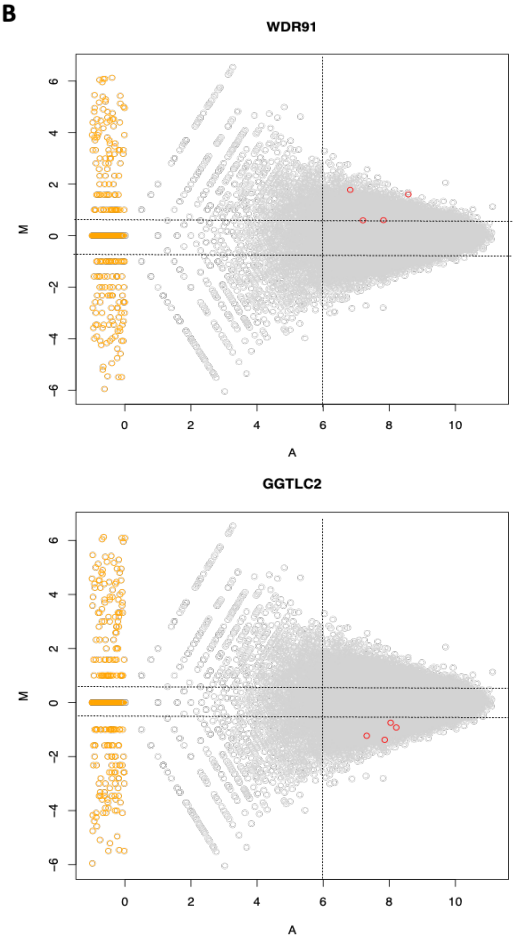

C

	Normalized Read counts		
sgRNA	CTL	TRT	Fold change
sgCOG8-1	110	204	1,854545455
sgCOG8-3	83	152	1,831325301
sgCOG8-4	85	165	1,941176471
sgWBSCR16-1	57	160	2,807017544
sgWBSCR16-2	107	204	1,906542056
sgWBSCR16-3	43	116	2,697674419
sgWBSCR16-4	156	360	2,307692308
sgWDR91-1	61	209	3,426229508
sgWDR91-3	219	664	3,03196347
sgGGTLC2-1	244	104	2,346153846
sgGGTLC2-2	375	144	2,604166667
sgGGTLC2-3	408	215	1,897674419
sgGGTLC2-4	341	203	1,679802956

Figure 4

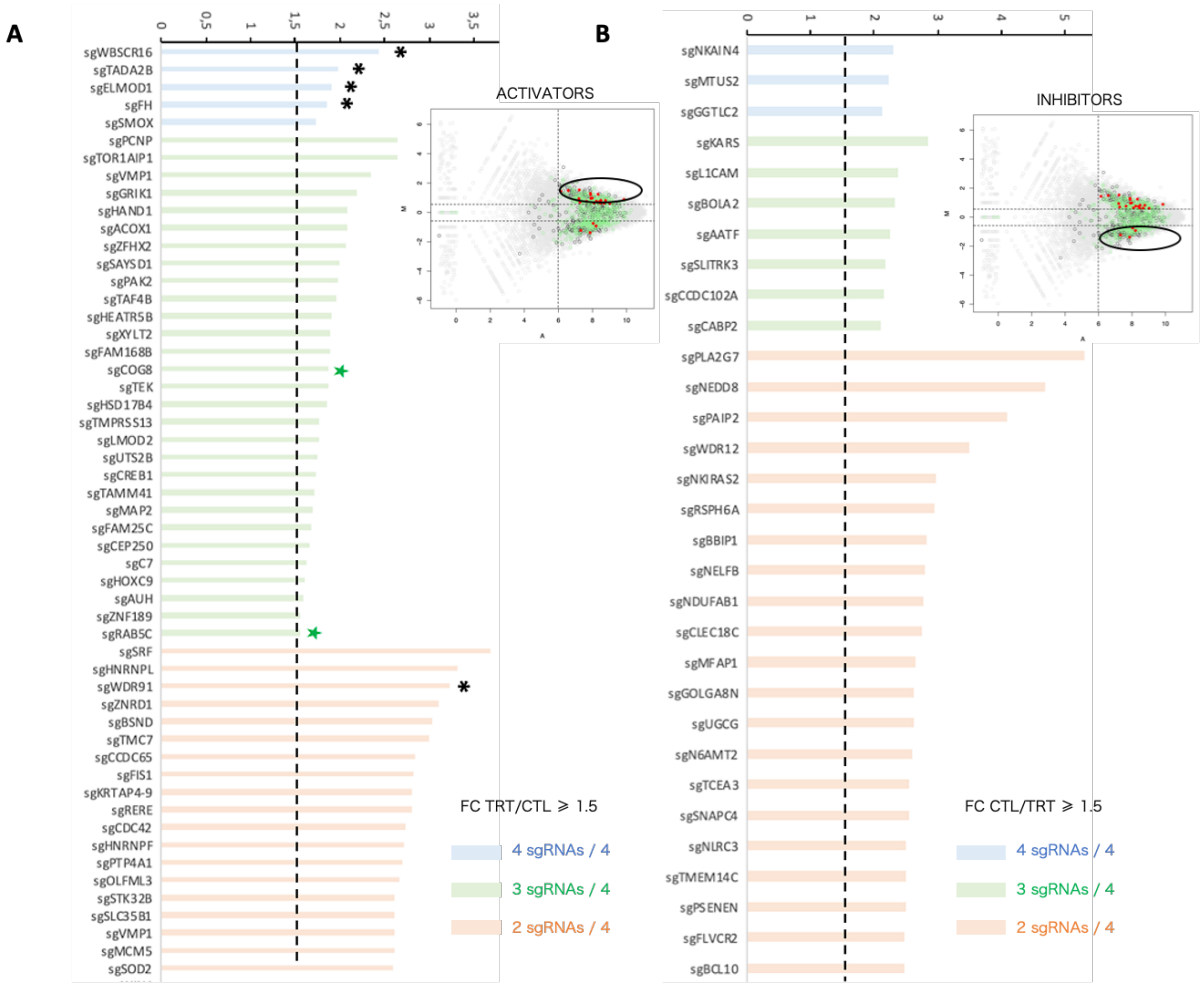
A
B
ACTIVATORS
INHIBITORS
FC TRT/CTL ≥ 1.5
FC CTL/TRT ≥ 1.5
4 sgRNAs / 4
3 sgRNAs / 4
2 sgRNAs / 4
sgWBSCR16
sgTADA2B
sgELMOD1
sgFH
sgSMOX
sgPCNP
sgTOR1AIP1
sgVMP1
sgGRIK1
sgHAND1
sgACOX1
sgZFHX2
sgSAYSD1
sgPAK2
sgTAF4B
sgHEATR5B
sgXYLT2
sgFAM168B
sgCOG8
sgTEK
sgHSD17B4
sgTMPRSS13
sgLMOD2
sgUTS2B
sgCREB1
sgTAMM41
sgMAP2
sgFAM25C
sgCEP250
sgC7
sgHOXC9
sgAUH
sgZNF189
sgRAB5C
sgSRF
sgHNRNPL
sgWDR91
sgZNRD1
sgBSND
sgTMC7
sgCCDC65
sgFIS1
sgKRTAP4-9
sgRERE
sgCDC42
sgHNRNPF
sgPTP4A1
sgOLFML3
sgSTK32B
sgSLC35B1
sgVMP1
sgMCM5
sgSOD2
sgNKAIN4
sgMTUS2
sgGGTLC2
sgKARS
sgL1CAM
sgBOLA2
sgAATF
sgSLITRK3
sgCCDC102A
sgCABP2
sgPLA2G7
sgNEDD8
sgPAIP2
sgWDR12
sgNKIRAS2
sgRSPH6A
sgBBIP1
sgNELFB
sgNDUFAB1
sgCLEC18C
sgMFAP1
sgGOLGA8N
sgUGCG
sgN6AMT2
sgTCEA3
sgSNAPC4
sgNLRC3
sgTMEM14C
sgPSENEN
sgFLVCR2
sgBCL10

Figure 5

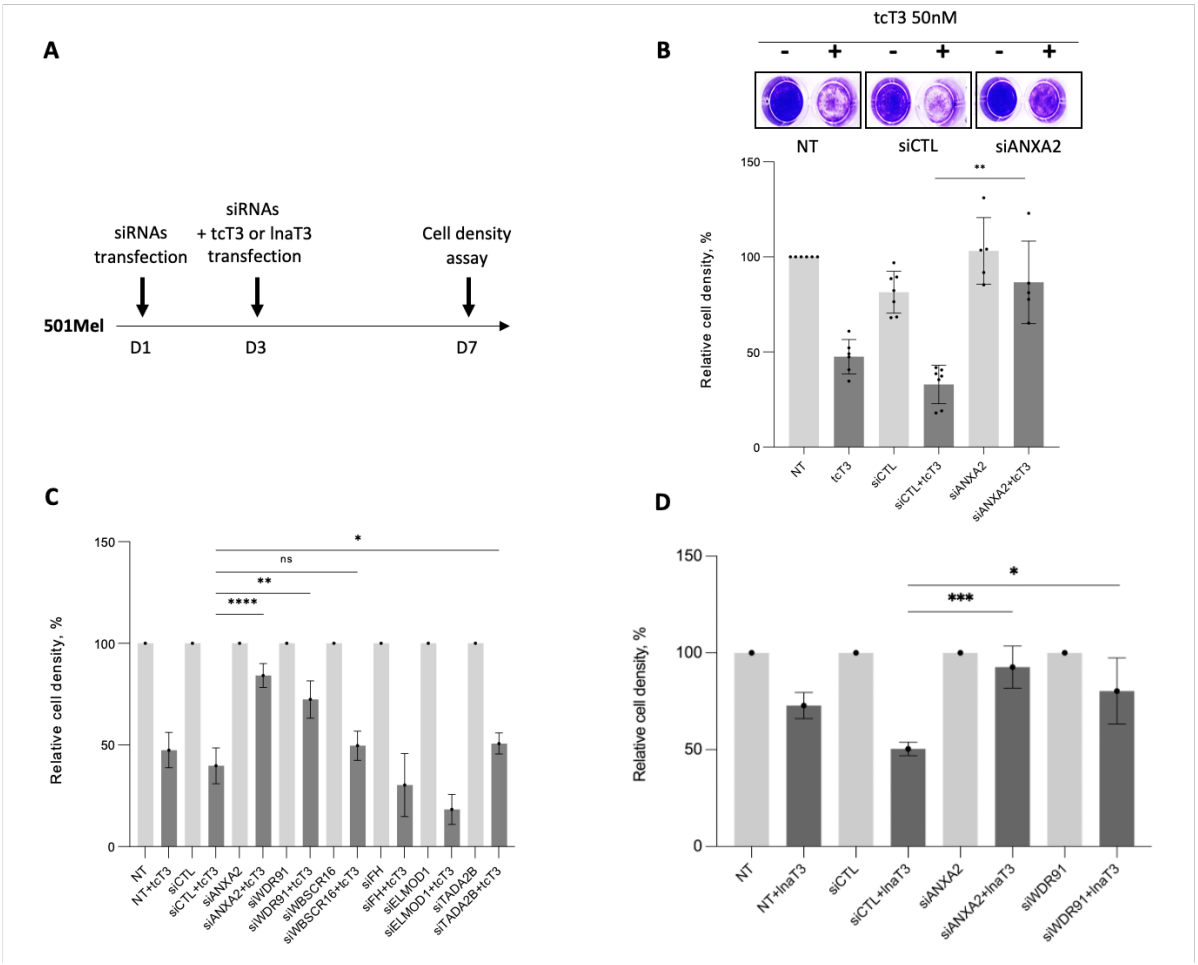
A
siRNAs transfection
siRNAs + tcT3 or lnaT3 transfection
Cell density assay
501Mel
D1
D3
D7
B
tcT3 50nM
- + - + - +
NT
siCTL
siANXA2
Relative cell density, %
150
100
50
0
**
NT
tcT3
siCTL
siCTL+tcT3
siANXA2
siANXA2+tcT3
C
Relative cell density, %
150
100
50
0
*
ns
**
****
NT
NT+tcT3
siCTL
siCTL+tcT3
siANXA2
siANXA2+tcT3
siWDR91
siWDR91+tcT3
siWBSCR16
siWBSCR16+tcT3
siFH
siFH+tcT3
siELMOD1
siELMOD1+tcT3
siTADA2B
siTADA2B+tcT3
D
Relative cell density, %
150
100
50
0
*
***
NT
NT+lnaT3
siCTL
siCTL+lnaT3
siANXA2
siANXA2+lnaT3
siWDR91
siWDR91+lnaT3

Figure 6

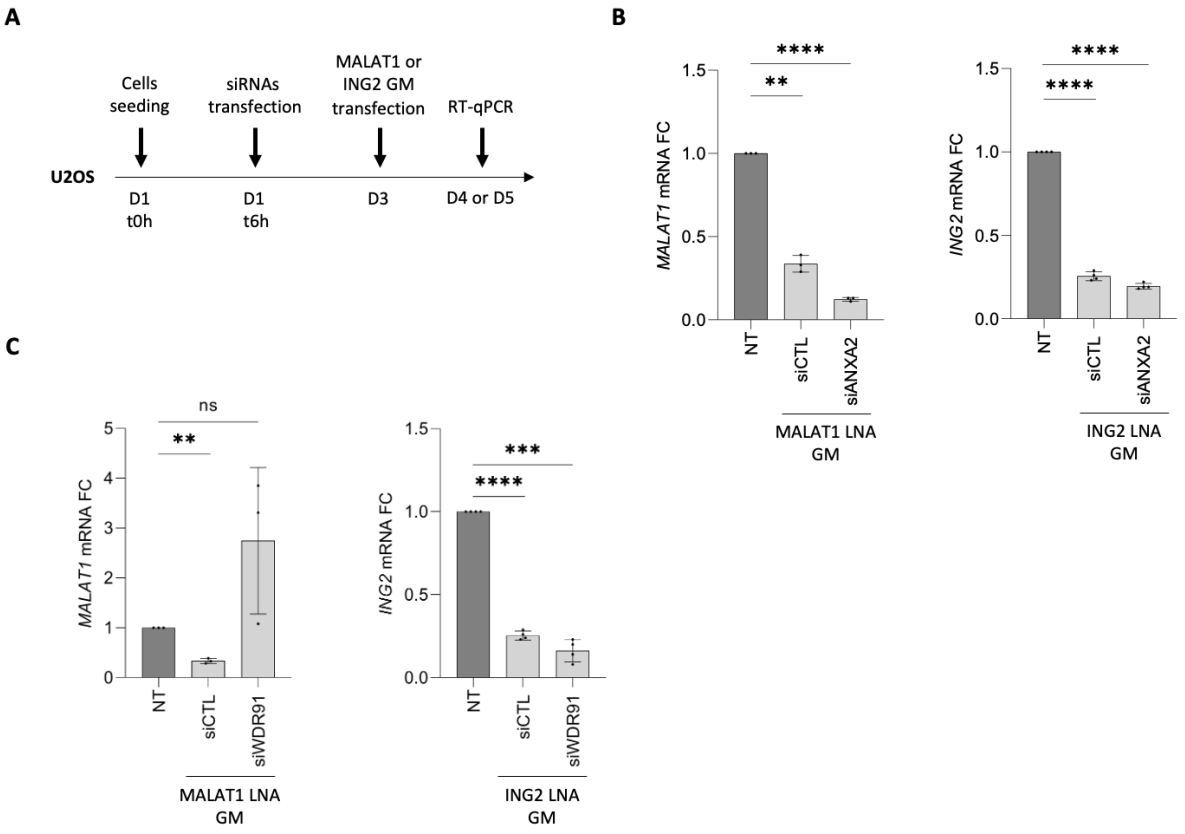
A
Cells seeding
siRNAs transfection
MALAT1 or ING2 GM transfection
RT-qPCR
U2OS
D1 t0h
D1 t6h
D3
D4 or D5
B
MALAT1 mRNA FC
ING2 mRNA FC
NT
siCTL
siANXA2
MALAT1 LNA GM
ING2 LNA GM
C
ns
**
***
****
siWDR91
MALAT1 LNA GM
ING2 LNA GM

Figure 7

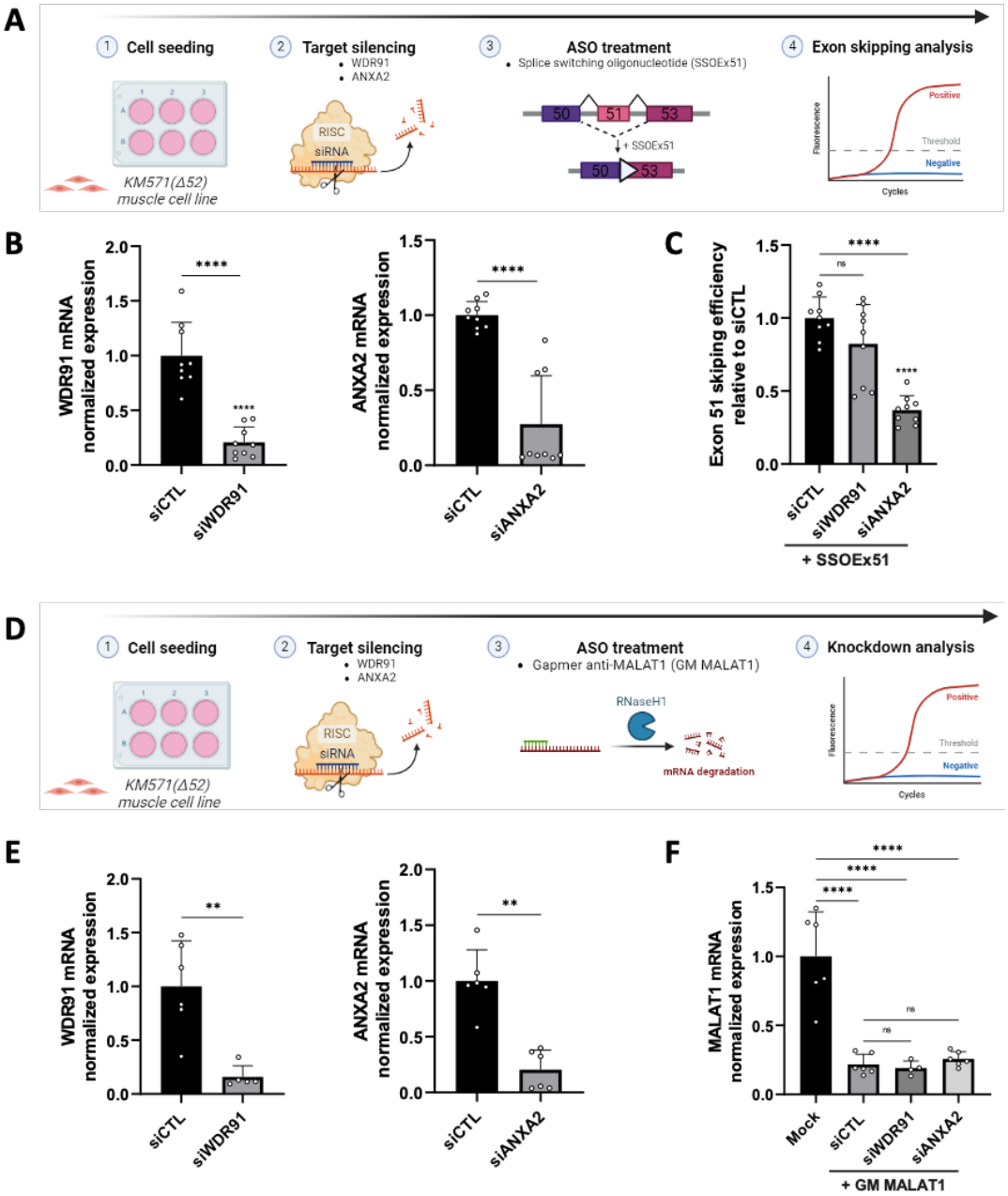
A
1 Cell seeding
2 Target silencing
• WDR91
• ANXA2
3 ASO treatment
• Splice switching oligonucleotide (SSOEx51)
4 Exon skipping analysis
KM571(Δ52) muscle cell line
RISC
siRNA
50
51
53
+ SSOEx51
Positive
Threshold
Negative
Fluorescence
Cycles
B
WDR91 mRNA normalized expression
ANXA2 mRNA normalized expression
siCTL
siWDR91
siANXA2
C
Exon 51 skiping efficiency relative to siCTL
+ SSOEx51
D
1 Cell seeding
2 Target silencing
• WDR91
• ANXA2
3 ASO treatment
• Gapmer anti-MALAT1 (GM MALAT1)
4 Knockdown analysis
RNaseH1
mRNA degradation
KM571(Δ52) muscle cell line
E
F
MALAT1 mRNA normalized expression
Mock
+ GM MALAT1